Diversity of fish sound types in the Pearl River Estuary, China

Authors

Zhi-Tao Wang [1*], Douglas P. Nowacek[2,3],TomonariAkamatsu[4],Ke-Xiong Wang [1], Jian-Chang Liu[5], Guo-Qin Duan[6], Han-Jiang Cao[6], Ding Wang [1]

[1] The Key Laboratory of Aquatic Biodiversity and Conservation of the Chinese Academy of Sciences, Institute of Hydrobiology of the Chinese Academy of Sciences, Wuhan, P. R. China

[2] Division of Marine Science and Conservation, Nicholas School of the Environment, Duke University of Marine Laboratory, Beaufort, NC, USA

[3] Pratt School of Engineering, Duke University, Durham, NC, USA

[4]National Research Institute of Fisheries Science, Fisheries Research and Development Agency, Kanagawa, Japan

[5] Transport Planning and Research Institute, Ministry of Transport, Beijing, P. R. China

[6] Hong Kong-Zhuhai-Macao Bridge Authority, Guangzhou, P. R. China

[*] also at Nicholas School of the Environment, Duke University, Beaufort, NC, USA

Corresponding Authors:

Ke-Xiong Wang and Ding Wang

7# Donghu South Road, Wuhan, Hubei, 430074, China

Email addresses: wangk@ihb.ac.cn (K.X.W.); wangd@ihb.ac.cn (D.W.)

Abstract

Background. Repetitive species-specific sound enables the identification of the presence and behavior of soniferous species by acoustic means. Passive acoustic monitoring has been widely applied to monitor the spatial and temporal occurrence and behavior of calling species.

Methods. Underwater biological sounds in the Pearl River Estuary, China, were collected using passive acoustic monitoring, with special attention paid to fish sounds. A total of 1408 suspected fish calls comprising 18,942 pulses were qualitatively analyzed using a customized acoustic analysis routine.

Results. We identified a diversity of 66 types of fish sounds. In addition to single pulse, the sounds tended to have a pulse train structure. The pulses were characterized by an approximate 8 ms duration, with a peak frequency from 500 to 2600 Hz and a majority of the energy below 4000 Hz. The median inter-pulsepeak interval (IPPI) of most call types was 9 or 10 ms. Most call types with median IPPIs of 9 ms and 10 ms were observed at times that were exclusive from each other, suggesting that they might be produced by different species. According to the literature, the 1+1 and $1+N_{10}$ call types might belong to big-snout croaker (*Johnius macrorhynus*), and $1+N_{19}$ might be produced by Belanger's croaker (*J. belangerii*).

Discussion. Categorization of the baseline ambient biological sound is an important first step in mapping the spatial and temporal patterns of soniferous fishes. The next step is the identification of the species producing each sound. The distribution pattern of soniferous fishes will be helpful for the protection and management of local fishery resources and in marine environmental impact assessment. Since the local vulnerable Indo-Pacific humpback dolphin (*Sousa chinensis*) mainly preys on soniferous fishes, the fine-scale distribution pattern of soniferous fishes can aid in the

Commented [MLJ1]: I don't know what these are – is there another way of explaining the types more simply?

conservation of this species. Additionally, prey and predator relationships can be observed when a database of species-identified sounds is completed.

Keywords: Hierarchical cluster analysis, Indo-Pacific humpback dolphins, Passive acoustic monitoring, Pearl River Estuary, Pulse train, Fish sound

Running title: Diversity of fish sounds in China

Introduction

The Pearl River Estuary (21°40′-22°50′ N; 112°50′-114°30′E) is in a subtropical area of the northern South China Sea. The estuary is one of the most economically developed regions in China, and the rapid local industrialization and large-scale infrastructure projects, e.g., the ongoing construction of the Hong Kong-Zhuhai-Macao bridge (Wang et al. 2014b) and the Guishan wind farm project (Wang et al. 2015b), have placed an extraordinarily heavy burden on coastal environments and accelerated human damage to coastal ecosystems.

The Pearl River Estuary shelters the world's largest known population of Indo-Pacific humpback dolphins (*Sousa chinensis*, locally called the Chinese white dolphin) (Chen et al. 2010; Jefferson & Smith 2016; Preen 2004), with an estimated population of 2637 (Coefficient of variation of 19% to 89%) (Chen et al. 2010; Jefferson & Smith 2016). The general preference of this species for estuarine habitats and coastal and shallow water (<30 m depth) distribution make it susceptible to the impacts of human activity (Jefferson & Smith 2016). The current conservation status of the Chinese white dolphin meets the IUCN Red List criteria for classification as Vulnerable; however, the conservation management in a majority of its distribution range is severely inadequate, and the humpback dolphin population in the Pearl River Estuary is declining by 2.5% annually (Karczmarski et al. 2016). A combination of fisheries entanglement and habitat degradation/loss have contributed to its population decline, along with contributions from pollution and anthropogenic noise disturbances (Jefferson & Smith 2016; Karczmarski et al. 2016). The magnitude of the threats will increase as land reclamation and sewage discharge continue to expand in the future in addition to the rapid local industrialization. Thus, concerns regarding the conservation of the local humpback dolphin population are increasing.

The humpback dolphin appears to rely almost exclusively on fish for food (Barros et al. 2004; Parra & Jedensjö 2014). Its prey includes the fish families of Sciaenidae (croakers), Engraulidae (anchovies), Trichiuridae (cutlassfish), Clupeidae (sardines), Ariidae(sea catfish) and Mugilidae (mullets)(Barros et al. 2004; Parra &Jedensjö 2014). Notably, the majority of these species are soniferous fishes (Banner 1972; Fish & Mowbray 1970; Ren et al. 2007; Whitehead & Blaxter 1989). The top three most important and frequent prey of humpback dolphins in the Pearl River Estuary are the brackish water species of croaker (*Johnius sp.*), spiny-head croaker (*Collichthys lucidus*), and anchovies (*Thryssa spp*., *T. dussumieri* and/or *T. kammalensis*) (Barros et al. 2004). The former two are soniferous fishes (Ren et al. 2007), and the latter might be capable of making sounds(Whitehead & Blaxter 1989). Additionally, it has been proposed that dolphins rely heavily on eavesdropping (passive listening)(Barros 1993; de Oliveira Santos et al. 2002)during the search phase of the foraging process(Gannon et al. 2005).

Sound production in soniferous fish has been shown to be associated with reproduction (e.g., courtship and spawning) and territorial or aggressive behavior(Hawkins & Amorim 2000; Takemura et al. 1978). Most of the repetitive fish sounds are species specific (Tavolga 1964), which enables the identification of the distribution and behavior of soniferous species by acoustic means. As a noninvasive technology, passive acoustic monitoring has been widely applied to map the spatial (over a wide range of habitats and at varied depths)(Wall et al. 2012; Wall et al. 2013) and temporal (diel, seasonal and annual) (Locascio & Mann 2011; Ruppé et al. 2015; Turnure et al. 2015) occurrence and behaviors of soniferous fishes, even in severe conditions, such as the presence of harmful algal blooms (Wall et al. 2014)or during hurricanes(Locascio & Mann 2005).

Overfishing and ocean pollution in the past decade have led to a dramatic decrease in fish in the

Commented [MLJ2]: I think this section above is too long – it is background to why you are doing the study on the soniferous fish and should be a sentence or two – possibly better in the discussion.

Commented [MLJ3]: Start of introduction

Commented [MLJ4]: Is this relevant?

wild fisheries of China(Liu & Sadovy 2008; Sadovy & Cheung 2003). The endemic species of giant yellow croaker (*Bahaba taipingensis*), which is highly valued for the medicinal properties of its swim bladder and was an important fish stock before the 1960s, collapsed in the wild and was determined to be commercially extinct in 1997(Sadovy & Cheung 2003). The spotted drum (*Nibea diacanthus*) and large yellow croaker (*Pseudosciaena crocea*, which is endemic to East Asia and was once one of the three top commercial marine fishes in China), have been severely depleted throughout their geographic range since the 1980s and have now almost entirely disappeared from landings (Liu & Sadovy 2008; Sadovy & Cheung 2003). The most recent study of humpback dolphin biosonar activity in the Pearl River Estuary indicated that its diel, seasonal and tidal patterns might be ascribed to the spatial-temporal variability of its prey (Wang et al. 2015b); however, little attention has been paid to local fishes, with only sporadic fishery distribution data with poor temporal and spatial resolution obtained from 1986-1987 by bottom trawl and in 1998 by beam trawl and hang trawl(Li et al. 2000b; Wang & Lin 2006). The fine-scale distribution pattern of humpback dolphin prey has yet to be investigated.

In this study, the ambient biological sounds in the Pearl River Estuary were recorded using passive acoustic monitoring. Suspected fish sounds were quantitatively and qualitatively characterized. We compared the species-specific (signature) sounds thorough a literature review, especially of those species that are distributed in the research area, to confirm the caller's identity. These baseline data can serve as a first step toward mapping the spatial and temporal patterns of soniferous fishes. Moreover, they are helpful for planning fisheries management and evaluation of the damage to aquatic environments from various large-scale infrastructure projects because marine environmental impact assessments must be based upon a good understanding of the local baseline

Commented [MLJ5]: Most people would argue that these are fictional! "Valued as a traditional medicine"? maybe?

Commented [MLJ6]: Both species or only the latter?

biodiversity. Additionally, the baseline data can aid in the protection of local humpback dolphins and the implementation of conservation strategies.

Methods

Acoustic data recording system

Underwater acoustic recordings were made using a Song Meter Marine Recorder (Wildlife Acoustics, Inc., Maynard, MA, USA), which included an HTI piezoelectric omnidirectional hydrophone (model HTI-96-MIN; High Tech, Inc., Long Beach, MS, USA) with a sensitivity of -164 dB re 1 V/µPa at 1 m distance, a recording bandwidth of 2Hz-48kHz and a flat frequency response over a wide range of 2 Hz-37 kHz (±3 dB). The hydrophone also included a programmable autonomous signal processing unit integrated with a band-pass filter and a pre-amplifier. The signal processing unit can log data at a resolution of 16 bits and at a 96 kHz sampling rate, with a storage capacity of 512 GB. The signal processing unit was sealed inside a water proof PVC housing and was submersible to 150 m. The recording system was calibrated prior to shipment from the manufacturer.

Data collection

Static acoustic monitoring was conducted underwater at the base of a telephone signal tower (22°07′54″ N, 113°43′54″ E) located among the Sanjiao, Chitan and Datou islands (Fig. 1).The recordings were taken continuously throughout deployment periods from May 26 to June 4, 2014, and June 17 to 22, 2014, at a 96 kHz sampling rate. The acoustic recording system was attached to a steel wire rope and suspended below the signal tower in the middle of water column 4.0 m above the ocean floor and approximately 3.0 to 5.8 m (depending on the tide conditions) below the water

surface. A 40 kg anchor block was attached on the bottom of the steel wire rope and laid down on the seabed to reduce the movement of the recording system due to water currents.

Acoustic data analysis

Upon retrieval of the recorder, the acoustic data were downloaded and processed, Raven Pro Bioacoustics Software (version 1.4; Cornell Laboratory of Ornithology, NY, USA) was used to initially visualize the acoustic data in the spectrogram (window type: Hann windows; fast Fourier transform (FFT) size: 2048 samples; frame overlapping: 80%; frequency grid spacing: 46.88 Hz; temporal grid resolution: 4.26 ms). Only calls with good signal-to-noise ratios (SNR > 15dB, noise level obtained just before or after the pulse) and satisfying the criteria of no interference by other sounds were extracted for further quantitative analyses. To make the data more independent and reduce the possibility of using multiple sounds from the same individual, only one signal was extracted for each call type in every 10 min bin for further analysis.

Deleted: during off-line signal processing

The recorded sounds generally featured single or multiple-pulse structures. A custom acoustic analysis routine based on MATLAB 7.11.0 (The Mathworks, Natick, MA, USA) was developed to analyze the extracted calls. For each call, the peak amplitude time for each pulse within the call was logged using a pulse-peak detector. Through trial and error, the pulse was defined and extracted as an 8 ms signal that began 2.5 ms before and ended 5.5 ms after the time point of the peak amplitude (Fig. 2B and C). The 8 ms definition was validated because it encompassed the majority of the energy of a pulse and was longer than the shortest interval between pulses within a call. The sonic parameters of the number of pulses in a call, total call duration (in ms, derived by adding 8 ms to the time difference of the last pulsepeak and the first pulsepeak), inter-pulsepeak interval (IPPI, the

158 time difference between the peak amplitude of consecutive pulse units in the train, which is equal
159 to the pulse period in the literature (Parmentier et al. 2009)), and the inter-pulse interval (IPI, the
160 time interval between the end of one pulse and the onset of the next one in a series) were calculated
161 for each call. The temporal characteristics for each 8 ms pulse were computed as $\tau_{95\%}$, τ_{-3dB} and τ_{-10dB}. $\tau_{95\%}$ is the duration containing 95% of the cumulative energy of the pulse (Fig. 2D), which
163 began when 2.5% of the cumulative signal energy was reached ($CE_{2.5\%}$in Fig. 2D) and ended when
164 97.5% of the cumulative signal energy was reached ($CE_{97.5\%}$ in Fig. 2D), and τ_{-3dB} and τ_{-10dB} are the
165 time differences between the end points that were 3 dB and 10 dB lower than the peak amplitude of
166 the envelope of the pulse waveform, respectively (Fig. 2E). The signal envelope was generated by
167 taking the absolute value of the waveform after applying the Hilbert transform function (Au 1993;
168 Madsen & Wahlberg 2007). The frequency and bandwidth properties for each 8 ms pulse were
169 determined from the power spectrum, which was calculated from the squared fast Fourier transform
170 of a 96,000-point Hanning window. Because the parameters of 3-dB and 10-dB bandwidths might
171 only cover the frequency range near the peak frequency and tend to provide a misrepresentation of
172 the bandwidth of signals with bimodal spectra (Au 2004), as was the case here, in addition to the
173 peak frequency (f_p, the frequency at which the spectrum has its maximum value) (Fig. 2F), we
174 measured the center frequency (f_c, the frequency that divides the power spectrum into equal energy
175 halves) and centralized root-mean-square bandwidth (BW_{rms}, the spectral standard deviation of the
176 f_c of the spectrum)(Au 1993; Madsen & Wahlberg 2007), which were proposed to be good
177 descriptive parameters for signals with bimodal spectra (Au 2004). The quality factor of each pulse
178 (Q, an appropriate way to define the relative width of a signal) was computed as the ratio of the f_c
179 to the BW_{rms}(Au 1993; Au 2004). The sound pressure levels (SPLs, dB re 1μPa) and energy flux

Commented [MLJ7]: This is a long and complicated sentence – consider turning it into a table of definitions?

Commented [MLJ8]: Split this into at least 2 sentences!

density (EFD, dB re 1μPa^{2}s) were derived for each 8 ms pulse over its $\tau_{95\%}$. The SPL parameters included the zero-to-peak SPL (SPL_{zp}) and the root-mean-square SPL (SPL_{rms}) (Urick 1983). The absolute pressure levels were derived by subtracting the sensitivity of the hydrophone and the gain due to the amplifier(Urick 1983).

The pooled distribution pattern of the IPPI for all analyzed calls was characterized by a multi-peak mode, with a distribution curve peaking at 9, 10, 12, 13 and 18 ms (Fig. 3A). Previous experience in fish acoustic analysis by other investigators indicated that the IPPI was the most reliable basis for signal identification and species-specific recognition (Mann & Lobel 1997; Parmentier et al. 2009; Spanier 1979), and most signals in our database ended with a pulse train featuring regular IPPIs (Table 1). In this study, calls were classified into types primarily based on their IPPI patterns and their amplitude and temporal modulation patterns(Table 1). The calls were initially grouped according to the number of sections they contained (Table 1). For each call, pulses with IPPIs greater than 1.5 times the median IPPI of the call were divided into different sections. Based on the bimodal distribution of the IPPI for calls that consisted of fewer than three pulses, pulses with an IPPI greater than 24 ms (three times the duration of a single pulse of 8 ms) were divided into different sections (Fig. 3B). To name each call type, such as $2+1+N_{10}$, $(1\text{-})^4+(2\text{-})^2+N_{10}$ and ${}^{i}N_{13}$, '+' was used to separate the different sections of a call, a number was used to denote the number of pulse for that section and '(1-)' and '(2-)' to denote repeated sections that consist of one or two pulses, respectively, with digital superscripts denoting the number of repeats in a repeating section. 'N' was used to denote the last section of a call with a variable number of pulses, and the digital subscripts denote the median IPPIs of the last portion of the call; the subscript i was used to denote calls with a zero-to-peak sound pressure level of the first pulse approximately 10 dB weaker

than that of the remainder of the call. Occasionally, a train of calls was extracted with significantly higher SNR (SNR>25dB), a regular inter-call interval, and a gradually changing pattern in its sound pressure level distinct from the ambient biological sounds. These sounds were likely produced by the same individual fish, which facilitated the estimation of the inter-call intervals.

Commented [MLJ9]: I think it would be helpful to have this illustrated in a graphic.

Statistical analysis

Descriptive statistics were used to summarize the biographical information. All the parameters were tested for normality (using the Shapiro–Wilk test for data sets < 50 or the Kolmogorov–Smirnov test for data sets ≥ 50) and homoscedasticity (using Levene's test for equality of variance) (Zar 1999). Because of the grossly skewed distribution of the majority of the data, the descriptive parameters of median, quartile deviation (QD), 5th percentile (P5), and 95th percentile (P95) were adopted. The QD was defined as one-half the interquartile range, which is the difference between the 25th and 75th percentiles in a frequency distribution.

Principal component analysis was used to identify the variables explaining the most variance among the acoustic parameters. Call types with an analyzed number greater than five were extracted for further discriminant and cluster analyses. Canonical discriminant analysis was used to assess the variation among call types relative to the variation within call types and determine the validity of our call types. Hierarchical cluster analysis (Romesburg 2004), a step-wise process that merges the two closest or furthest data points at each step and builds a hierarchy of clusters based on the distance between them, was applied to discover similar call types in each set. Because the amplitude parameters were not critical for species recognition (Ha 1973) and the call duration was dependent on the number of pulses in a call (Parmentier et al. 2009), these parameters were not included in the

principal component analysis, canonical discriminant analysis and hierarchical cluster analysis. The statistical analyses were performed using Statistical Package for the Social Sciences 16.0 for Windows (SPSS Inc., Chicago, IL, USA).

Results

Over 16 recording days, ambient biological sounds and suspected fish sounds were recorded daily and sometimes formed dense choruses of individual sound emissions produced simultaneously and/or overlapping with each other that obscured the signals and could not be discriminated individually, especially before dusk. In addition to some single pulses, individual calls tended to possess a multi-pulse burst structure. The most representative pulse consisted of 6 oscillations (Fig. 2C). Owing to the single hydrophone methodology, animal localization was not possible in this study. The recorded sound was occasionally clipped, indicating that the source level of the sound was higher than 164 dB (limited by the hydrophone sensitivity). A total of 1408 calls comprising 18,942 pulses were extracted for statistical analysis and were categorized into 66 call types (Table 1).

Single-section calls

Calls that consisted of a single section included call types 1 (Table S1), 2 (Table S1, Fig.S1), N_9 (Table 2, Fig.4), N_{10} (Table 2, Fig.4), N_{13} (Table 2, Fig.5), N_{17} (Table 2, Fig.4), $^{i}N_{13}$ (Table 3, Fig.5) and $^{i}N_{15}$ (Table 3, Fig.5).

Two-section calls

Calls consisting of two sections included call types 1+1 (Table S1, Fig.S1), 1+N_{10} (Table 4, Fig.6), 1+N_{12} (Table 4, Fig.6), 1+N_{19} (Table 4, Fig.6), 2+N_9 (Table S2, Fig.S2), 2+N_{10} (Table S2, Fig.S2), 2+N_{18} (Table S2, Fig.S2), 3+N_9 (Table S3, Fig.S3), 3+N_{10} (Table S3, Fig.S3), 3+N_{17} (Table S3, Fig.S3), 4+N_9 (Table S4, Fig.S4), 4+N_{10} (Table S4, Fig.S4), 4+N_{17} (Table S4, Fig.S4), and 5+N_{10} (Table S5, Fig.S5).

Three-section calls

Calls consisting of three sections included call types $(1-)^2$+N_9 (Table S6, Fig.S6), $(1-)^2$+N_{10} (Table S6, Fig.S6), $(1-)^2$+N_{12} (Table S6, Fig.S6), 1+2+N_{10} (Table S7, Fig.S7), 1+2+N_{18} (Table S7, Fig.S7), 2+1+N_9 (Table S8, Fig.S8), 2+1+N_{10} (Table S8, Fig.S8), $(2-)^2$+N_{10} (Table S9, Fig.S9), 3+1+N_9 (Table S10, Fig.S10), 3+1+N_{10} (Table S10, Fig.S10), 3+2+N_9 (Table S11, Fig.S11) and 4+1+N_{10} (Table S9, Fig.S9).

Four-section calls

Calls consisting of four sections included call types $(1-)^3$+N_9 (Table S12, Fig.S12), $(1-)^3$+N_{10} (Table S12, Fig.S12), $(1-)^3$+N_{12} (Table S12, Fig.S12), $(1-)^2$+2+N_9 (Table S13, Fig.S13), $(1-)^2$+2+N_{10} (Table S13, Fig.S13), $(1-)^2$+3+N_{10} (Table S14, Fig.S14), 2+$(1-)^2$+N_9 (Table S15, Fig.S15), 2+$(1-)^2$+N_{10} (Table S15, Fig.S15), 2+1+2+N_9 (Table S16, Fig.S16), 2+1+2+N_{10} (Table S16, Fig.S16) and 3+$(1-)^2$+N_9 (Table S11, Fig.S11).

Five-section calls

Calls consisting of five sections included call types $(1-)^4$+N_9 (Table S17, Fig.S17), $(1-)^4$+N_{10} (Table S17, Fig.S17), $(1-)^4$+N_{12} (Table S17, Fig.S17), $(1-)^3$+2+N_{10} (Table S18, Fig.S18), $(1-)^3$+3+N_{10} (Table S18, Fig.S18), $(1-)^2$+2+1+N_{10} (Table S19, Fig.S19), $(1-)^2$+2+3+N_{10} (Table S19, Fig.S19), and 2+$(1-)^3$+N_{10} (Table S20, Fig.S20).

Six-section calls

Calls consisting of six sections included call types $(1\text{-})^5+N_9$ (Table S21 and Fig.S21), $(1\text{-})^5+N_{10}$ (Table S21 and Fig.S21), $(1\text{-})^4+2+N_{10}$ (Table S22 and Fig.S22), $(1\text{-})^4+3+N_{11}$ (Table S22 and Fig.S22), $(1\text{-})^3+2+1+N_{10}$ (Table S23 and Fig.S23), and $2+(1\text{-})^4+N_{10}$ (Table S20, Fig.S20).

Seven-section calls

Calls consisting of seven sections included call types $(1\text{-})^6+N_{10}$ (Table S24 and Fig.S24), $(1\text{-})^5+2+N_{10}$ (Table S25 and Fig.S25), $(1\text{-})^5+3+N_{10}$ (Table S25 and Fig.S25), $(1\text{-})^4+2+1+N_{10}$ (Table S23 and Fig.S23), and $(1\text{-})^4+(2\text{-})^2+N_{10}$ (Table S26 and Fig.S24).

Eight-section calls

Calls consisting of eight sections included call types $(1\text{-})^7+N_{10}$ (Table S24 and Fig.S24) and $(1\text{-})^5+(2\text{-})^2+N_{10}$ (Table S26 and Fig.S26).

Commented [MLJ10]: You need to find another way of presenting this. There is far too much detail here.

Principal component, discriminant function and hierarchical cluster analyses

The principal component analysis indicated that approximately 81.1% of the variability is explained by the first four principal components (39.2% by principal component 1, 18.1% by principal component 2, 13.2% by principal component 3, and 10.6% by principal component 4). Principal component 1 was loaded with the τ_{-3dB}, τ_{-10dB}, f_c, BW_{rms} and Q parameters. Principal component 2 was loaded with f_p. The third component describes the temporal parameter of the IPPI, and the fourth component describes the temporal parameters of τ_{-10dB} and the IPPI. The validity of our call types was confirmed using a canonical discriminant function that grouped N_{17}, $1+N_{19}$, $2+N_{18}$ and $3+N_{17}$ (Fig. 7A). Hierarchical clustering using a between-groups linkage method that measures the squared Euclidean distance automatically grouped the 31 extracted call types into five

clusters. The N_{17}, $1+N_{19}$, $2+N_{18}$ and $3+N_{17}$ call types were grouped into one cluster, and $^{i}N_{13}$ and $^{i}N_{15}$ were grouped together (Fig. 7B). Most of the call types with an IPPI median of 10 ms were grouped together, and those with an IPPI median of 9 ms were grouped together (Fig. 7B).

Call occurrence patterns

All call types with median IPPIs of 9 ms for the last section (i.e., call types with median IPPIs of 9 ms except the N_9 call type), including $2+N_9$, $3+N_9$, $4+N_9$, $(1-)^2+N_9$, $2+1+N_9$, $3+1+N_9$, $3+2+N_9$, $(1-)^3+N_9$, $(1-)^2+2+N_9$, $2+(1-)^2+N_9$, $2+1+2+N_9$, $3+(1-)^2+N_9$, $(1-)^4+N_9$, and $(1-)^5+N_9$, were only observed from June 18-20, 2014 (Fig. 8). Most of the call types with median IPPIs of 10 ms for the last section (88%, 29 out of 33), except $1+N_{10}$, $(1-)^2+N_{10}$, $1+2+N_{10}$, and $(1-)^3+N_{10}$, were only observed from May 26-June 4 and June 21-22, 2014 (Fig. 8).

Commented [MLJ11]: I think perhaps find another way of presenting this.

Characteristics of call trains

Of the 52 extracted call trains, the estimated inter-call interval was 1.88±0.39 ms (median±QD; P5–P95:1.05-3.04 ms, n=278).

Discussion

Fish sonic muscles are the fastest-contracting vertebrate muscles (Rome & Lindstedt 1998). Many soniferous fishes produce species-specific sounds by driving their swim bladders with the highly specialized sonic muscles during courtship to aggregate males and females and facilitate successful mating, especially at night and/or in highly turbid water(Fine & Parmentier 2015; Tavolga 1964). The spawning-related sounds produced by soniferous fishes have been widely used to identify the timing of spawning and map the areas where spawning occurs (Locascio & Mann 2011; Turnure et al. 2015). The sound recording period in our study was during the spawning seasons of a majority

of the local fishes because their reproduction behavior was most evident from March through June in the Pearl River Estuary (Sadovy 1998), e.g., the spawning activity of the greyfin croaker (*Pennahia anea*) occurred from March-April to June, with a peak in May(Tuuli et al. 2011), the spawning season of the spiny-head croaker began in March and lasted until December, and the season for Belanger's croaker (*Johnius belangerii*) was from April to December (Li et al. 2000a; Sadovy 1998).

In the present study, presumably spawning choruses were recorded daily, indicating that the sound recording location is a spawning place for local soniferous fish. The smallest inter-pulsepeak interval in our study was 8.32 ms, which was longer than and further validated the conservatively defined 8 ms pulse duration. In this study, the call types were categorized primarily by their IPPI patterns rather than the IPPI ranges, i.e., the range of IPPIs in different call types are not necessarily exclusive, as between the N_9 and N_{10} call types and between the $^{i}N_{13}$ and $^{i}N_{15}$ call types. Although there was some overlap in the range of IPPIs, N_9 and N_{10} (A4 and B4 in Fig. 4 and S27 Fig.) and $^{i}N_{13}$ and $^{i}N_{15}$ (A4 and B4 in Fig. 5) were separated based on the distribution pattern of their IPPIs.

Commented [MLJ12]: Too long!

Commented [MLJ13]: Too long!

Sound comparison of soniferous fish in the PRE

The South China Sea, with at least 2321 fish species belonging to 35 orders, 236 families and 822 genera(Ma et al. 2008), has long been recognized as a global center of marine tropical biodiversity (Barber et al. 2000) and is one of the richest areas in China, even globally, in terms of its marine fish diversity (Huang 1994; Ma et al. 2008). More than 834 fish species belonging to 25 orders, 124 families and 390 genera were recorded in the waters near Hong Kong(Ni & Kwok 1999).

Comparisons with Sciaenidae sounds

Fishes of the family Sciaenidae, which are commonly known as croakers or drums, are some of

the most well-studied soniferous fish species, and more than 23 species in this family were recorded in the waters near Hong Kong (Ni & Kwok 1999).

Voluntary sounds

In free-ranging conditions, big-snout croaker (*J. macrorhynus*) can emit voluntary purr signals with the first and the remaining IPPIs averaging 40.1 ms and 9.7 ms in the field and 35.3 ms and 10.4 ms in a large aquarium, respectively (Table 5)(Lin et al. 2007), which resembles the $1+N_{10}$ call type in our study (Table 4, Fig. 6A) (note that the IPPI was equal to the summation of the pulse duration and the inter-pulse interval in Lin et al. 2007). In addition, the peak frequency of the pulses in $1+N_{10}$ (mean ± sd: 1077 ± 244, N=1507) was intermediate between those in the pulses of big-snout croaker purr signals as recorded in the field (mean ± sd: 1146±131, N=250) and in a large aquarium (mean ±s d: 1050 ± 84, N=60). Additionally, the voluntary dual-knock signal of big-snout croaker with an average IPPI of 36.7 ms and 39.4 ms as recorded in the field and in a large aquarium, respectively (Table 5)(Lin et al. 2007), resembled the 1+1 call type in our study with an IPPI of 40.70±4.08 (mean±sd) (Table S1, Fig.S1B). These matches were further supported by the fact that the peak frequency of the pulses in the 1+1 call type (mean±sd: 1077.75±219.58, N=126) was close to that of the dual-knock recorded in the field (mean±sd: 1133±119, N=40) or a large aquarium (mean±sd: 1135±85, N=50).

Belanger's croaker can emit sounds with the first IPPI much longer than subsequent IPPIs, which follow at regular intervals of approximately 20 ms(Pilleri et al. 1982) and resemble the $1+N_{19}$ call type in our study, although the first IPPI in Belanger's croaker (approximately 40 ms) (Table 5) (Pilleri et al. 1982) was smaller than that in the $1+N_{19}$ call type (median at 71.36 ms) (Table 4, Fig. 6C). Their similarity was further strengthened by the fact that the temporal and frequency

353 characteristics of the signal emitted by Belanger's croaker, which consists of 4-14 pulses with a 140-
354 260 ms call duration, a 500-1000 Hz peak frequency and a majority of the energy within the 500-
355 4000 Hz frequency band (Pilleri et al. 1982), resemble those of the $1+N_{19}$ call type, which consists
356 of 3-12 pulses with a 97.37-272.85 ms call duration and peak frequency median of approximately
357 789 Hz (Table 4).

358 Sounds from the white croaker (*Pennahia argentata*) (Ramcharitar et al. 2006; Takemura et al.
359 1978), southern meagre (*Argyrosomus japonicus*)(Ueng et al. 2007), yellow drum (*Nibea albiflora*)
360 (Ren et al. 2007)(Ramcharitar et al. 2006; Takemura et al. 1978), Reeve's croaker (*N. acuta* or
361 *Chrysochir aureus*)(Trewavas 1971; Ren et al. 2007) and large yellow croaker(Liu et al. 2010; Ren
362 et al. 2007) were also compared. However, these sounds (Table 5) did not match any call types in
363 our study based on their temporal and/or frequency characteristics.

364 Belanger's croaker can also emit long bursts with a peak frequency of 750-1250 Hz (Pilleri et al.
365 1982), and a chorus sound of unknown species recorded in Xiamen Harbor of East China Sea from
366 1981-1982 with sound energy concentrated in the 700-1600 Hz frequency band and a peak
367 frequency of 1250 Hz was proposed to be emitted by Belanger's croaker(Zhang et al. 1984). Chorus
368 sounds of the genus *Johnius* (possibly *J. fasciatus* or *J. amblycephalus*) and the genus *Pennahia*
369 (possibly *P. miichthioides*) recorded in the Bohai Sea and Yellow Sea from 1989-1990 were also
370 reported. The sounds emitted by the former genus have an average peak frequency of 2000 Hz and
371 a majority of energy concentrated in the 1000-4000 Hz frequency band, whereas the sounds emitted
372 by the latter genus have an average peak frequency of 400 Hz and majority of energy concentrated
373 in the 200-800 Hz frequency band (Xu & Qi 1999). Chorus sounds of the spiny-head croaker were
374 recorded in the South China Sea in 1967, with a majority of energy concentrated in the 500-1250

Deleted:)

Deleted: (

Hz frequency band and a peak frequency of approximately 1000 Hz (Qi et al. 1982), and chorus sounds of unknown species recorded in the adjacent waters of Xiamen Harbor of the East China Sea from 1981-1982, with sound energy concentrated in the 700-1600 Hz frequency band and peak frequencies of 800 Hz and 1000 Hz, were ascribed to the spiny-head croaker(Zhang et al. 1984). However, detailed waveform, spectrum and statistical results for the temporal and frequency characteristics of individual sounds in these choruses were not available, preventing direct comparison with our study.

Disturbance sound

Sound recorded under disturbance, e.g., under hand-held conditions is possibly not significantly different from those recorded under voluntary conditions and can be employed to match the sound in the field (Lin et al. 2007). We also compared the disturbance sound of the species distributed in our study region, including Belanger's croaker(Mok et al. 2011a), big-snout croaker(Lin et al. 2007; Mok et al. 2011a), Sciaenidae *J. distincus*(Mok et al. 2011a; Tsai 2009), sin croaker (*J. dussumieri*) (Tsai 2009), white croaker(Mok et al. 2011a), greyfin croaker(Mok et al. 2011a), bighead white croaker (*P. macrocephalus*) (Mok et al. 2011a), pawak croaker (*P. pawak*) (Mok et al. 2011a), Reeve's croaker (Tsai 2009), tiger-toothed croaker (*Otolithes ruber*) (Mok et al. 2011a), and blackmouth croaker (*Atrobucca nibe*) (Mok et al. 2011a). However, these signals (Table 5) did not match any call types in our study.

Comparison with other soniferous fish families

Soundsfrom other soniferous fish families, including cutlassfish (*Trichiurus haumela*, family: Trichiuridae)(Ren et al. 2007), elongate ilisha (*Ilisha elongata*, family: Pristigasteridae)(Ren et al. 2007), sea catfish (*Arius sp.* and *A. maculates*, family: Ariidae)(Mok et al. 2011a; Ren et al. 2007),

Commented [MLJ14]: Too long

Commented [MLJ15]: Just cite these two references at the end of the sentence.

Commented [MLJ16]: You need to illustrate how they did not match. Where are the data? What are the differences?

399 pearl perch (*Glaucosoma buergeri*, family: Glaucosomatidae)(Mok et al. 2011b), bigeye snapper
400 (*Priacanthus macracanthus*, family: Priacanthidae)(Tsai 2009), trumpeter perch (*Pelates*
401 *quadrilineatus*, family: Terapontidae) (Tsai 2009) and javelin grunter (*Pomadasys kaakan*, family:
402 Haemulidae)(Tsai 2009), were also compared with our call types but did not match (Table 5) any
403 call types in our study.

Commented [MLJ17]: You need to say more about/illustrate how they did not match – perhaps a table?

404 ## Comparison with other passive acoustic monitoring sounds

405 The statistical parameters of the eight types of wild fish sounds recorded in seven estuaries of the
406 west coast of Taiwan using passive acoustics were unfortunately not available, which restricted
407 direct comparison(Mok et al. 2011a). However, the general trend of the $1+N_{10}$ and $1+N_{12}$ call types
408 in our study resembles their type B signal (Mok et al. 2011a), with the first inter-pulse interval much
409 longer than the following ones that had a non-increasing inter-pulse interval toward the end of the
410 call, and the N_{17} call type in our study resembles their type E signal (Mok et al. 2011a), with a
411 gradually increasing inter-pulse interval toward the end of the call and the sound energy
412 concentrated in discrete bands. Sounds with much longer second or third inter-pulse intervals, which
413 resemble our 2+N and 3+N, respectively, were also observed in the Chosui River in Taiwan (Mok
414 et al. 2011a), but the sound producer was not identified.

415 ## Occurrence pattern of call types

416 In the field environment, to communicate without misinterpreting the messages and to avoid
417 jamming, different species of a fish community will partition the underwater acoustic environment
418 (Ruppé et al. 2015). In our study, most call types with IPPI medians at 9 ms and 10 ms were observed
419 at times that were exclusive from each other, suggesting they might have been produced by different
420 species.

Additional studies with more controlled conditions, such as in an aquarium or with field recording equipped with a high-definition sonar system such as the DIDSON Dual-frequency Identification Sonar system, will be required to identify the species producing the calls in our study.

Call trains

Due to the relative simplicity of vocal mechanisms and lack of ability to produce complex calls, fish typically emit sounds with variation in either the temporal and/or frequency patterning (Rice & Bass 2009). Additionally, the temporal and spectral characteristics of fish signals are involved in information coding and are important parameters for the recognition of sound in fishes(Malavasi et al. 2008; Spanier 1979). In the present study, fish sounds tended to be frequency modulated, e.g., the peak frequency of the pulses within a call were variable (Fig. 2F), and amplitude modulated, e.g., the $^{i}N_{13}$ and $^{i}N_{15}$ call types. This is possible because the amplitude of the sound is determined by the swim bladder(Fine et al. 2001; Tavolga 1964) and the dominant frequency of the signal is determined by the sonic muscle twitch duration and the forced response of the swim bladder to sonic muscle contractions rather than the natural resonant frequency of the swim bladder(Connaughton et al. 2002).

Passive hearing by the dolphin

In addition to emitting high-frequency pulsed sounds for echolocation and navigation, humpback dolphins can produce narrow-band, frequency-modulated whistles with a fundamental frequency range of 520-33,000 Hz(Wang et al. 2013) and apparent source levels of 137.4 ± 6.9 dB re 1μPa in rms(Wang et al. 2016) for communication. The fish sounds recorded in this study, which were characterized by a peak frequency between 500 and 2600 Hz and a maximum zero-to-peak sound pressure level greater than 164 dB, were well within the frequency range of humpback dolphin

443 whistles. It is highly probable that the fish sounds function as acoustic clues of prey to the dolphin,
444 i.e., the dolphin relies heavily on passive hearing during the search phase of the foraging process.
445 This passive hearing mechanism of the local humpback dolphin is further reinforced by the fact that
446 the brackish water species of *C. lucidus* and tapertail anchovy (*Coilia mystus*, Family: Engraulidae)
447 were the top two predominant species in the seawater/freshwater mixing zones of the Pearl River
448 Estuary(Zhan 1998), accounting for 89% and 72% of the numbers and biomass, respectively, of the
449 whole fish stock in the Pearl River Estuary region (Wang & Lin 2006). The soniferous fish *C.*
450 *lucidus* was observed to be the second-most important prey for humpback dolphin, but the non-
451 soniferous fish *C. mystus* was not identified in their prey spectrum(Barros et al. 2004).
452

453 # Importance and application

454 The high biodiversity of fish fauna in the Pearl River Estuary is a treasure of genetic resources
455 and has great potential application value. However, the loss of the fishery stocks over time has been
456 devastating. Historically poor management and overfishing of wild stocks of the large yellow
457 croaker resulted in overwhelming collapses throughout its geographic range, and although
458 substantial funds have been provided and many remedial actions such as fishery control, restocking
459 and marine aquaculture have been applied. However, aquaculture can only supplement, rather than
460 substitute for, wild fisheries(Goldburg & Naylor 2005). No evidence of recovery in the wild stock
461 of large yellow croaker has been observed, and its genetic diversity continues to decrease(Liu &
462 Sadovy 2008). Similar lessons can be learned from the Atlantic salmon (*Salmo salar*) (Goldburg &
463 Naylor 2005). Given the sharp declines in fish stocks, especially of the larger species of croakers
464 owing to overfishing in the Pearl River Estuary, and given that fishing pressure is still high and may

be even higher in the future, management activities such as more effective fishing moratoriums should be applied to protect the remaining croakers and other fisheries during the spawning season, especially at their spawning grounds. The baseline data of the ambient biological acoustics in our study represent a first step toward mapping the spatial and temporal patterns of soniferous fishes and are helpful for the protection, management and effective utilization of fishery resources. In addition, since marine environmental impact assessment must be based upon a good understanding of the local biodiversity, the baseline data of suspected fish sounds in our study can facilitate the evaluation of the impacts from various infrastructure projects on local aquatic environments by comparing the baseline to post-construction and/or post-mitigation effort data. Additionally, there is a large body of evidence that the distribution pattern of marine mammals tends to be correlated with the spatial-temporal variability of their prey (Benoit-Bird & Au 2003; Wang et al. 2015a; Wang et al. 2014a); this correlation was also proposed for the vulnerable local humpback dolphin(Wang et al. 2015b), and the fine-scale distribution pattern of soniferous fishes can aid in the conservation of these emblematic dolphins.

Conclusion

Using passive acoustic monitoring, the ambient biological sounds in the Pearl River Estuary were recorded and analyzed. In addition to single pulse, the sounds tend to possess a pulse train structure with a peak frequency between 500 and 2600 Hz and most of the energy below 4000 Hz. Sixty-six call types were identified based on the number of sections, temporal characteristics and amplitude modulation patterns. Most of the call types with IPPI medians at 9 ms and those with medians at 10 ms were observed at times that were exclusive from each other, suggesting that they might be

487 produced by different species. A literature review suggested that the 1+1 and 1+N_{10} call types might
488 belong to big-snout croaker (*Johnius macrorhynus*) and 1+N_{19} might be produced by Belanger's
489 croaker (*J. belangerii*). The baseline data of suspected fish sounds in our study can facilitate the
490 evaluation of the impact from various infrastructure projects on the local aquatic environments by
491 comparing the baseline to post-construction and/or post-mitigation effort data, and the fine-scale
492 distribution pattern of soniferous fishes can aid in the conservation of the local vulnerable humpback
493 dolphins.
494

495 Acknowledgments

496 We gratefully acknowledge Wenjun Xu of the Ningbo No.2 High School in Zhejiang Province
497 for her statistical assistance. Special thanks are also extended to Andrew J. Read of the Duke
498 University Marine Laboratory for his helpful discussion about this study.

499 References

500 Au WWL. 1993. *The sonar of dolphins*. New York: Springer-Verlag.
501 Au WWL. 2004. Echolocation signals of wild dolphins. *Acoustical Physics* 50:454-462.
502 Banner A. 1972. Use of sound in predation by young lemon sharks, Negaprion brevirostris (Poey).
503 *Bulletin of Marine Science* 22:251-283.
504 Barber PH, Palumbi SR, Erdmann MV, and Moosa MK. 2000. Biogeography: a marine Wallace's
505 line? *Nature* 406:692-693.
506 Barros NB. 1993. Feeding ecology and foraging strategies of bottlenose dolphins on the central east
507 coast of Florida Ph.D.thesis. University of Miami.
508 Barros NB, Jefferson TA, and Parsons ECM. 2004. Feeding habits of Indo-Pacific humpback
509 dolphins (Sousa chinensis) stranded in Hong Kong. *Aquatic Mammals* 30: 179-188.
510 Benoit-Bird KJ, and Au WW. 2003. Prey dynamics affect foraging by a pelagic predator (Stenella
511 longirostris) over a range of spatial and temporal scales. *Behavioral Ecology and*

512 *Sociobiology* 53:364-373.
513 Chen T, Hung SK, Qiu YS, Jia XP, and Jefferson TA. 2010. Distribution, abundance, and individual
514 movements of Indo-Pacific humpback dolphins (Sousa chinensis) in the Pearl River Estuary,
515 China. *Mammalia* 74:117-125. 10.1515/Mamm.2010.024
516 Connaughton MA, Fine ML, and Taylor MH. 2002. Weakfish sonic muscle: influence of size,
517 temperature and season. *Journal of experimental biology* 205:2183-2188.
518 de Oliveira Santos MC, Rosso S, dos Santos RA, Lucato S, and Bassoi M. 2002. Insights on small
519 cetacean feeding habits in southeastern Brazil. *Aquatic Mammals* 28:38-45.
520 Fine ML, Malloy KL, King C, Mitchell SL, and Cameron TM. 2001. Movement and sound
521 generation by the toadfish swimbladder. *Journal of comparative Physiology A* 187:371-379.
522 Fine ML, and Parmentier E. 2015. Mechanisms of Fish Sound Production. In: Ladich F, ed. *Sound*
523 *Communication in Fishes*: Springer Vienna, 77-126.
524 Fish MP, and Mowbray WH. 1970. *Sound of western North Atlantic fishes*. Baltimore and London:
525 The Johns Hopkins Press.
526 Gannon DP, Barros NB, Nowacek DP, Read AJ, Waples DM, and Wells RS. 2005. Prey detection
527 by bottlenose dolphins, Tursiops truncatus: an experimental test of the passive listening
528 hypothesis. *Animal Behaviour* 69:709-720.
529 http://dx.doi.org/10.1016/j.anbehav.2004.06.020
530 Goldburg R, and Naylor R. 2005. Future seascapes, fishing, and fish farming. *Frontiers in Ecology*
531 *and the Environment* 3:21-28. 10.1890/1540-9295(2005)003[0021:FSFAFF]2.0.CO;2
532 Ha SJ. 1973. Aspects of sound communication in the damselfish Eupomacentrus partitus Ph.D.
533 Thesis. University of Miami.
534 Hawkins A, and Amorim MC. 2000. Spawning Sounds of the Male Haddock, Melanogrammus
535 aeglefinus. *Environmental Biology of Fishes* 59:29-41. 10.1023/A:1007615517287
536 Huang ZG. 1994. *Marine species and their distributions in China seas*. Beijing: China Ocean Press.
537 Jefferson TA, and Smith BD. 2016. Re-assessment of the Conservation Status of the Indo-Pacific
538 Humpback Dolphin (Sousa chinensis) Using the IUCN Red List Criteria. *Advances in*
539 *Marine Biology*: Academic Press, 1-26.
540 Karczmarski L, Huang S-L, Or CKM, Gui D, Chan SCY, Lin W, Porter L, Wong W-H, Zheng R,
541 Ho Y-W, Chui SYS, Tiongson AJC, Mo Y, Chang W-L, Kwok JHW, Tang RWK, Lee ATL,

Yiu S-W, Keith M, Gailey G, and Wu Y. 2016. Humpback Dolphins in Hong Kong and the Pearl River Delta: Status, Threats and Conservation Challenges. *Advances in Marine Biology*: Academic Press, 27–64.

Li Y, Chen G, and Sun D. 2000a. Analysis of the composition of fishes in the Pearl River estuarine waters. *Journal of fisheries of china* 24:312-317 (in chinese with english abstract).

Li Y, Chen G, and Sun D. 2000b. Analysis of the composition of fishes in the Pearl River estuarine waters. *Journal of fisheries of china* 24:312-317(in chinese with english abstract).

Lin YC, Mok HK, and Huang BQ. 2007. Sound characteristics of big-snout croaker, Johnius macrorhynus (Sciaenidae). *The Journal of the Acoustical Society of America* 121:586-593. doi:http://dx.doi.org/10.1121/1.2384844

Liu M, and Sadovy Y. 2008. Profile of a fishery collapse: why mariculture failed to save the large yellow croaker. *Fish and Fisheries* 9:219-242. 10.1111/j.1467-2979.2008.00278.x

Liu ZW, Xu XM, and Qin LH. 2010. Sound characteristics of the large yellow croaker, Pseudosciaena crocea (Sciaenidae). *Technical Acoustics* 29:342-343 (in chinese with english abstract).

Locascio JV, and Mann DA. 2005. Effects of Hurricane Charley on fish chorusing. *Biology Letters* 1:362-365. 10.1098/rsbl.2005.0309

Locascio JV, and Mann DA. 2011. Diel and seasonal timing of sound production by black drum (Pogonias cromis). *Fishery Bulletin* 109:327-338.

Ma C, You K, Zhang M, Li F, and Chen D. 2008. A preliminary study on the diversity of fish species and marine fish faunas of the South China Sea. *Journal of Ocean University of China* 7:210-214. 10.1007/s11802-008-0210-2

Madsen PT, and Wahlberg M. 2007. Recording and quantification of ultrasonic echolocation clicks from free-ranging toothed whales. *Deep Sea Research Part I: Oceanographic Research Papers* 54:1421-1444. 10.1016/j.dsr.2007.04.020

Malavasi S, Collatuzzo S, and Torricelli P. 2008. Interspecific variation of acoustic signals in Mediterranean gobies (Perciformes, Gobiidae): comparative analysis and evolutionary outlook. *Biological Journal of the Linnean Society* 93:763-778.

Mann DA, and Lobel PS. 1997. Propagation of damselfish (Pomacentridae) courtship sounds. *The Journal of the Acoustical Society of America* 101:3783-3791.

572 doi:http://dx.doi.org/10.1121/1.418425
573 Mok H-K, Lin S-Y, and Tsai K-E. 2011a. Underwater ambient biological noise in the waters on the
574 west coast of Taiwan. *Kuroshio Science* 5-1:51-57.
575 Mok H-K, Parmentier E, Chiu K-H, Tsai K-E, Chiu P-H, and Fine M. 2011b. An Intermediate in the
576 evolution of superfast sonic muscles. *Frontiers in Zoology* 8:31.
577 Ni I-H, and Kwok K-Y. 1999. Marine fish fauna in Hong Kong waters. *Zoological studies* 38:130-
578 152.
579 Parmentier E, Lecchini D, Frederich B, Brie C, and Mann D. 2009. Sound production in four
580 damselfish (Dascyllus) species: phyletic relationships? *Biological Journal of the Linnean*
581 *Society* 97:928-940. 10.1111/j.1095-8312.2009.01260.x
582 Parra GJ, and Jedensjö M. 2014. Stomach contents of Australian snubfin (Orcaella heinsohni) and
583 Indo-Pacific humpback dolphins (Sousa chinensis). *Marine Mammal Science* 30:1184-
584 1198. 10.1111/mms.12088
585 Pilleri G, Kraus C, and Gihr M. 1982. The ambient noise in the environment of Sousa plumbea and
586 Neophocaena phocaenoides with special reference to the sounds of Johnius belangerii
587 (Pisces, Sciaenidae). *Investigations on cetacea* 14:95-128.
588 Preen A. 2004. Distribution, abundance and conservation status of dugongs and dolphins in the
589 southern and western Arabian Gulf. *Biological Conservation* 118:205-218.
590 Qi ME, Zhang SZ, and Song ZX. 1982. The sound production of Collichthys aggregation.
591 *Oceanologia ET Limnologia Sinica* 13:491-495.
592 Ramcharitar J, Gannon DP, and Popper AN. 2006. Bioacoustics of fishes of the family Sciaenidae
593 (croakers and drums). *Transactions of the American Fisheries Society* 135:1409-1431.
594 Ren XM, Gao DZ, Yao YL, Yang F, Liu JF, and Xie FJ. 2007. Occurrence and characteristic of
595 sound in large yellow croaker (Pseudosciaena crocea). *Journal of Dalian fisheries*
596 *university* 22:123-128 (in chinese with english abstract).
597 Rice AN, and Bass AH. 2009. Novel vocal repertoire and paired swimbladders of the three-spined
598 toadfish, Batrachomoeus trispinosus: insights into the diversity of the Batrachoididae.
599 *Journal of experimental biology* 212:1377-1391.
600 Rome LC, and Lindstedt SL. 1998. The quest for speed: muscles built for high-frequency
601 contractions. *Physiology* 13:261-268.

602 Romesburg C. 2004. *Cluster analysis for researchers*. Raleigh, USA: Lulu Press.
603 Ruppé L, Clément G, Herrel A, Ballesta L, Décamps T, Kéver L, and Parmentier E. 2015.
604 Environmental constraints drive the partitioning of the soundscape in fishes. *Proceedings*
605 *of the National Academy of Sciences* 112:6092-6097. 10.1073/pnas.1424667112
606 Sadovy Y. 1998. Patterns of reproduction in marine fishes of Hong Kong and adjacent waters. In:
607 B.Morton, editor. Proceedings of the third international conference on the marine biology
608 of the south China sea, Hong kong. Hongkong: Hong Kong University Press. p 261-273.
609 Sadovy Y, and Cheung WL. 2003. Near extinction of a highly fecund fish: the one that nearly got
610 away. *Fish and Fisheries* 4:86-99.
611 Spanier E. 1979. Aspects of Species Recognition by Sound in Four Species of Damselfishes, Genus
612 Eupomacentrus (Pisces: Pomacentridae). *Zeitschrift für Tierpsychologie* 51:301-316.
613 10.1111/j.1439-0310.1979.tb00691.x
614 Takemura A, Takita T, and Mizue K. 1978. Studies on the underwater sound-Ⅶ: Underwater calls
615 of the Japanese marine drum fishes (Sciaenidae). *Bulletin of the Japanese Society of*
616 *Scientific Fisheries (Japan)* 44:121-125.
617 Tavolga WN. 1964. Sonic characteristics and mechanisms in marine fishes. In: Tavolga WN, ed.
618 *Marine Bio-acoustics*. New York: Pergamon Press, 195-211.
619 Trewavas E. 1971. The syntypes of the sciaenid Corvina albida Cuvier and the status of
620 Dendrophysa hooghliensis Sinha and Rao and Nibea coibor (nec Hamilton) of Chu, Lo &
621 Wu. *Journal of fish biology* 3:453-461.
622 Tsai K-E. 2009. Study of the acoustic characters of eleven soniferous fish in the western coastal
623 waters of Taiwan Master Master thesis. National Sun Yat-sen University.
624 Turnure JT, Grothues TM, and Able KW. 2015. Seasonal residency of adult weakfish (Cynoscion
625 regalis) in a small temperate estuary based on acoustic telemetry: a local perspective of a
626 coast wide phenomenon. *Environmental Biology of Fishes* 98:1207-1221.
627 Tuuli CD, De Mitcheson YS, and Liu M. 2011. Reproductive biology of the greyfin croaker
628 Pennahia anea in the northern South China Sea. *Ichthyological research* 58:302-309.
629 Ueng J-P, Huang B-Q, and Mok H-K. 2007. Sexual Differences in the Spawning Sounds of Japanese
630 Croaker, Argyrosomus japonicus (Sciaenidae). *Zoological studies* 46:103.
631 Urick RJ. 1983. *Principles of underwater sound*. New York: McGraw-Hill.

632 Wall CC, Lembke C, Hu C, and Mann DA. 2014. Fish Sound Production in the Presence of Harmful
633 Algal Blooms in the Eastern Gulf of Mexico. *PLOS ONE* 9:e114893.
634 10.1371/journal.pone.0114893
635 Wall CC, Lembke C, and Mann DA. 2012. Shelf-scale mapping of sound production by fishes in
636 the eastern Gulf of Mexico, using autonomous glider technology. *Marine Ecology Progress*
637 *Series* 449:55-64.
638 Wall CC, Simard P, Lembke C, and Mann DA. 2013. Large-scale passive acoustic monitoring of
639 fish sound production on the West Florida Shelf. *Marine Ecology Progress Series* 484:173-
640 188. 10.3354/meps10268
641 Wang D, and Lin SJ. 2006. Spatial and temporal variation of fish community structure in the Pearl
642 River Estuary waters. *South china fisheries science* 2:37-45(in chinese with english
643 abstract).
644 Wang Z-T, Akamatsu T, Mei Z-G, Dong L-j, Imaizumi T, Wang K-X, and Wang D. 2015a. Frequent
645 and prolonged nocturnal occupation of port areas by Yangtze finless porpoises
646 (Neophocaena asiaeorientalis): Forced choice for feeding? *Integrative zoology* 10:122-132.
647 10.1111/1749-4877.12102
648 Wang Z-T, Akamatsu T, Wang K-X, and Wang D. 2014a. The diel rhythms of biosonar behavior in
649 the Yangtze finless porpoise (Neophocaena asiaeorientalis asiaeorientalis) in the port of the
650 Yangtze river: The correlation between prey availability and boat traffic. *PloS one* 9:e97907.
651 10.1371/journal.pone.0097907
652 Wang Z-T, Au W, Rendell L, Wang K-X, Wu H-P, Wu Y-P, Liu J-C, Duan G-Q, Cao H-J, and Wang
653 D. 2016. Apparent source levels and active communication space of whistles of free-
654 ranging Indo-Pacific humpback dolphins (Sousa chinensis) in the Pearl River Estuary and
655 Beibu Gulf, China. *PeerJ* 4:e1695. 10.7717/peerj.1695
656 Wang Z-T, Fang L, Shi W-J, Wang K-X, and Wang D. 2013. Whistle characteristics of free-ranging
657 Indo-Pacific humpback dolphins (Sousa chinensis) in Sanniang Bay, China. *The Journal of*
658 *the Acoustical Society of America* 133:2479-2489. doi: 10.1121/1.4794390
659 Wang Z-T, Nachtigall PE, Akamatsu T, Wang K-X, Wu Y-P, Liu J-C, Duan G-Q, Cao H-J, and Wang
660 D. 2015b. Passive acoustic monitoring the diel, lunar, seasonal and tidal patterns in the
661 biosonar activity of the Indo-Pacific humpback dolphins (Sousa chinensis) in the Pearl

River Estuary, China. *PLOS ONE* 10:e0141807. doi: 10.1371/journal.pone.0141807

Wang Z-T, Wu Y-P, Duan G-Q, Cao H-J, Liu J-C, Wang K-X, and Wang D. 2014b. Assessing the underwater acoustics of the world's largest vibration hammer (OCTA-KONG) and its potential effects on the Indo-Pacific humpbacked dolphin (Sousa chinensis). *PLOS ONE* 9:e110590. doi: 10.1371/journal.pone.0110590

Whitehead PJP, and Blaxter JHS. 1989. Swimbladder form in clupeoid fishes. *Zoological Journal of the Linnean Society* 97:299-372. 10.1111/j.1096-3642.1989.tb00107.x

Xu LY, and Qi ME. 1999. Noise specctra of two fishes as observed in Bohai sea and Yellow sea. *Marine Sciences* 4:13-14.

Zar JH. 1999. *Biostatistical analysis* Upper Saddle River, NJ: Prentice-Hall.

Zhan HG. 1998. Study on fis community structure in the Zhujiang estuary and adjacent waters. *Acta Oceanologica Sinica* 20:91-97.

Zhang MQ, Shi XQ, Lin XQ, Li W, Ke LY, and Huang XD. 1984. Marine organism chorus obseved in Xiamen Harbor. *Acta Oceanologica Sinica* 6:10-15 (In chinese).

Figures and tables

Figure 1 Map of the passive acoustic monitoring area.

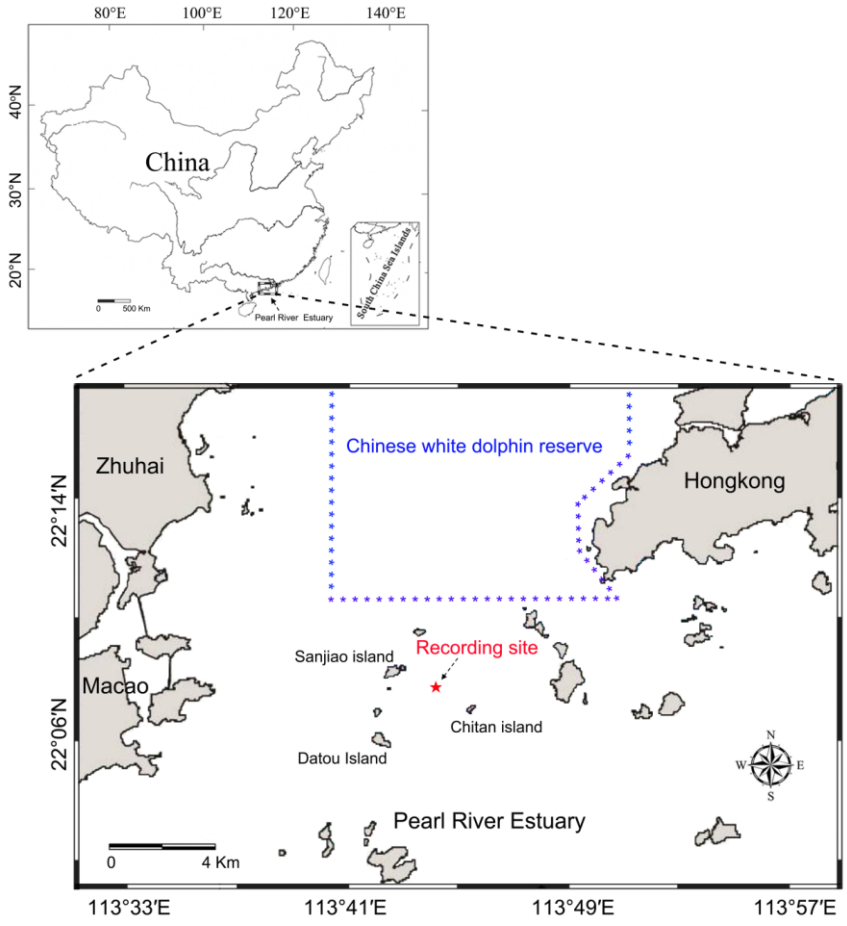

678

679 **Figure 2 Schematic diagram of the signal analysis.** (A) Oscillogram of the raw data with seven

680 pulses. (B) Pulses detected by the pulse-peak detector. Vertical dashed lines denote the starting

681 (green), peak (red), and ending (blue) points of a pulse. (C) Close-up of the oscillogram of extracted

682 8ms pulses showing the fine-scale call structure. (D) The cumulative energy of the extracted pulse,

683 $\tau_{95\%}$, was the duration containing 95% of the cumulative energy of the pulse, which was derived

684 from the time difference between the 2.5th and 97.5th cumulative energy percentiles. (E) Normalized

685 signal envelope of the extracted pulse; τ_{-3dB} and τ_{-10dB} are the time differences between the -3 dB

686 and -10 dB end points relative to the peak amplitude of the signal envelope, respectively. (F)

Normalized power spectrum of the extracted pulse. Spectrum configuration: FFT size, 96,000; frequency grid spacing, 1 Hz.

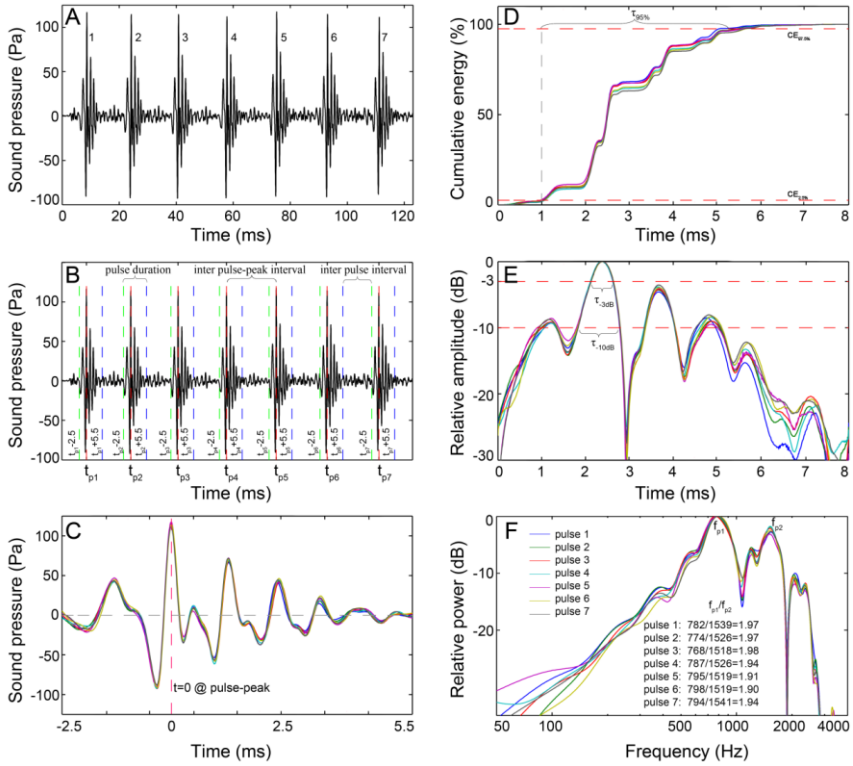

Figure 3 Distribution pattern of the inter-pulsepeak interval (IPPI) for all analyzed calls (A) and call types with fewer than three pulses (B). The distribution pattern of the pooled IPPIs peaked at 9, 10, 12,13 and 18 ms (inset figure in A). Call types with fewer than three pulses, including a two-pulse call in the 2, 1+1, 1+N_{19}, and $^{i}N_{13}$ call types and a three-pulse call in the $^{i}N_{13}$, N_{13}, N_{17}, and $(1\text{-})^{2}$+N_{10} call types. The bimodal distribution of the IPPI (inset figure in B) validated the selection of 24 ms, three times the duration of a single 8ms pulse, as a threshold for dividing pulses of a call into different sections. The insets show magnified time scales of the IPPI for 8-20 ms and 10-52 ms.

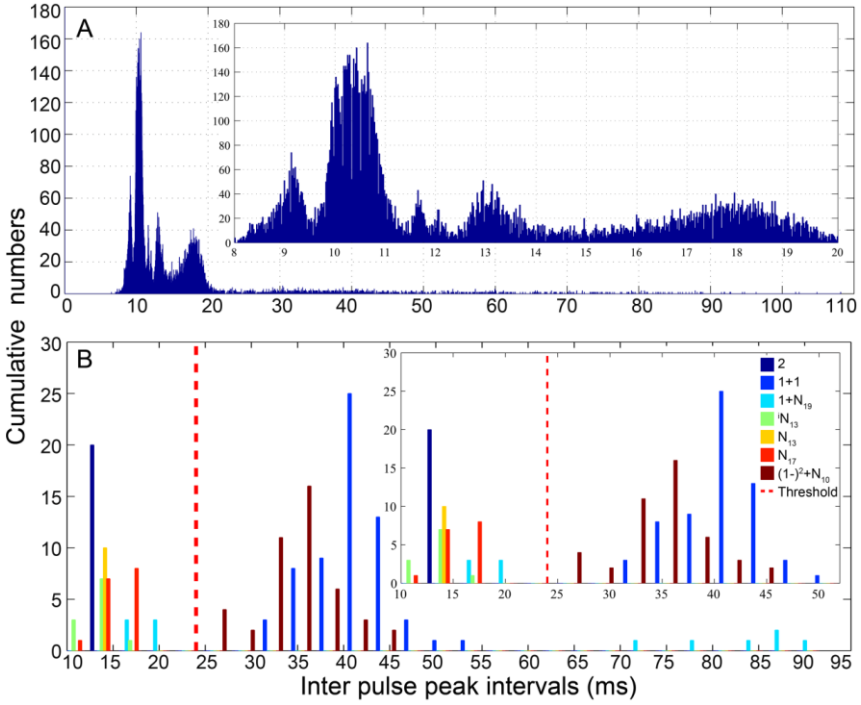

Figure 4 Characteristic of the (A) N_9, (B) N_{10}, (C) N_{13}, and (D) N_{17} call types. Rows 1 and 2 are the oscillogram and sonogram, respectively, of a representative signal for each call type. Row 3 is the duration of a call as a function of the number of pulses within the call. Rows 4-7 are the pooled inter-pulsepeak interval, sound pressure level, peak frequency, and center frequency of each pulse versus the order at which it occurs within a call, respectively. For the boxplot, the line inside the box indicates the median value, and the upper and lower box borders are the first and third quartiles, respectively. The length of the box is the interquartile range (IQR). The whiskers extend to the most extreme data within the limit of 1.5 IQRs from the end of the box. Open circles (o) denote mild outliers with values greater than 1.5 IQRs but fewer than 3 IQRs from the end of the box. Asterisks (*) denote extreme outliers with values greater than 3 box lengths from the upper or lower edges of the box. Sonogram configuration: FFT size, 96,000; window type, Hanning; overlap samples per

frame, 95%.

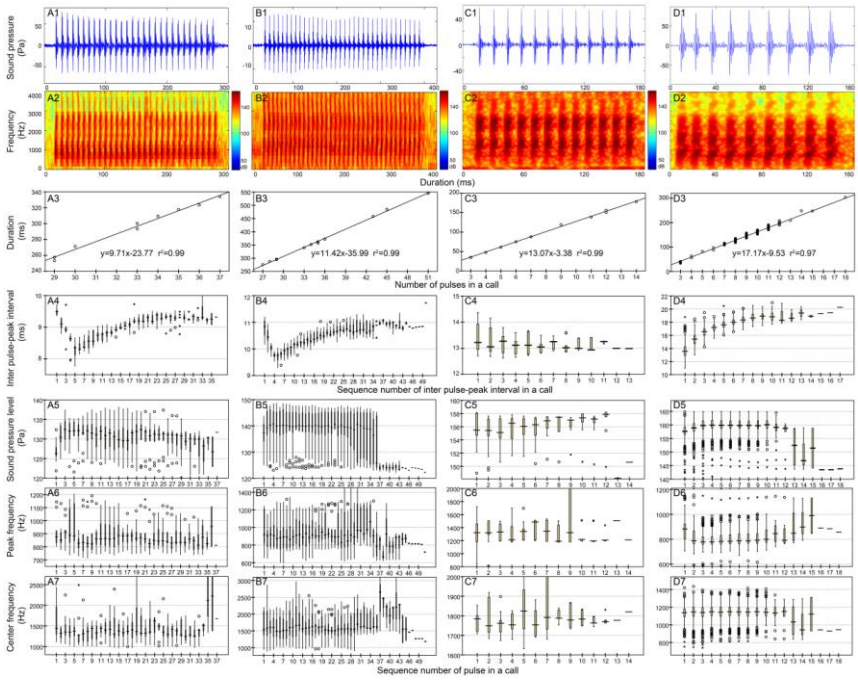

Figure 5 Characteristics of the (A) $^{i}N_{13}$ and (B) $^{i}N_{15}$ call types. Rows 1 and 2 are the oscillogram and sonogram, respectively, of a representative signal for each call type. Row 3 is the duration of a call as a function of the number of pulses within the call. Rows 4-7 are the pooled inter-pulsepeak interval, sound pressure level, peak frequency, and center frequency of each pulse versus the order at which it occurs within a call, respectively.

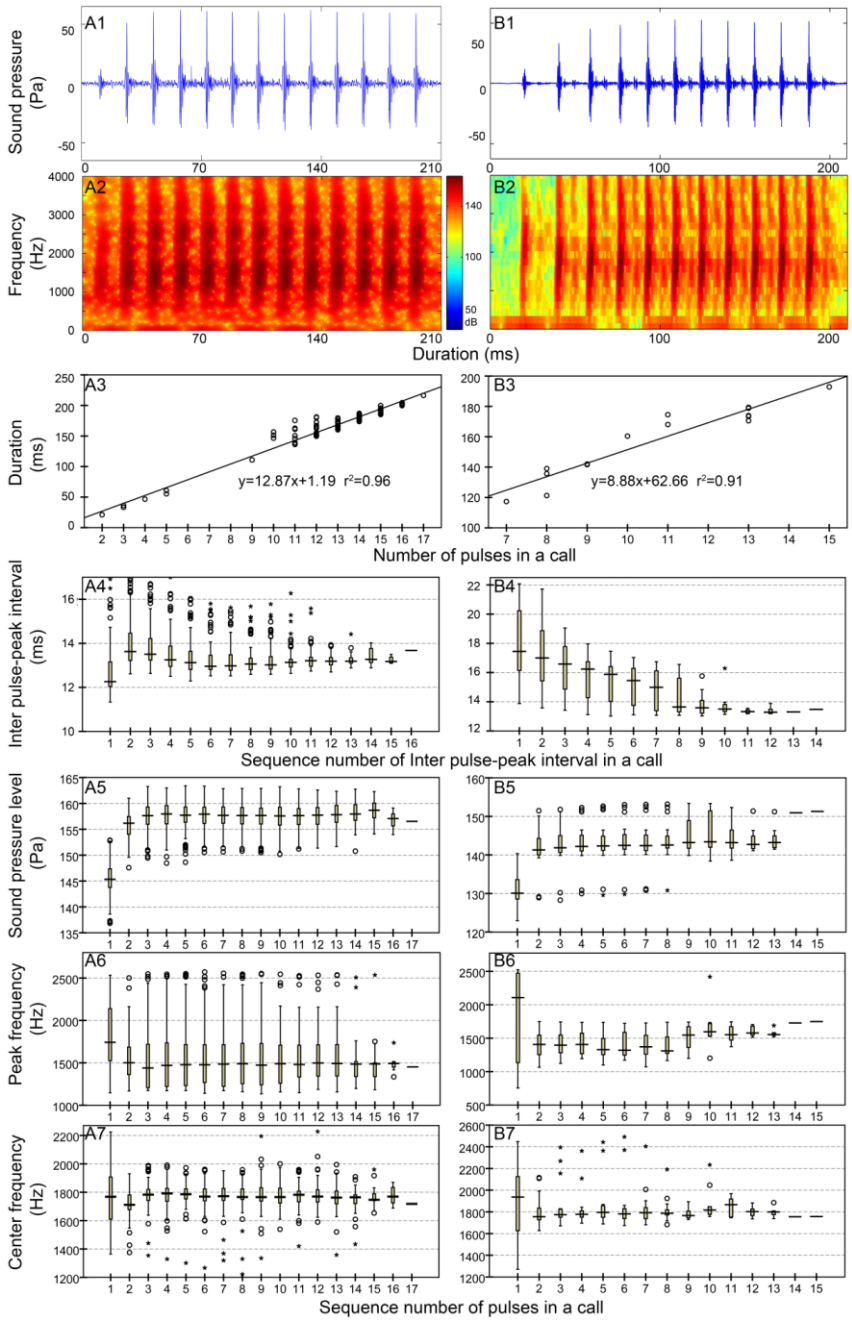

717

718 **Figure 6 Characteristics of the (A) 1+N_{10}, (B) 1+N_{12} and (C) 1+N_{19} call types.** Rows 1 and 2 are

719 the oscillogram and sonogram, respectively, of a representative signal for each call type. Row 3 is
720 the duration of a call as a function of the number of pulses within the call. Rows 4-7 are the pooled
721 inter-pulsepeak interval, sound pressure level, peak frequency, and center frequency of each pulse
722 versus the order at which it occurs within a call, respectively.

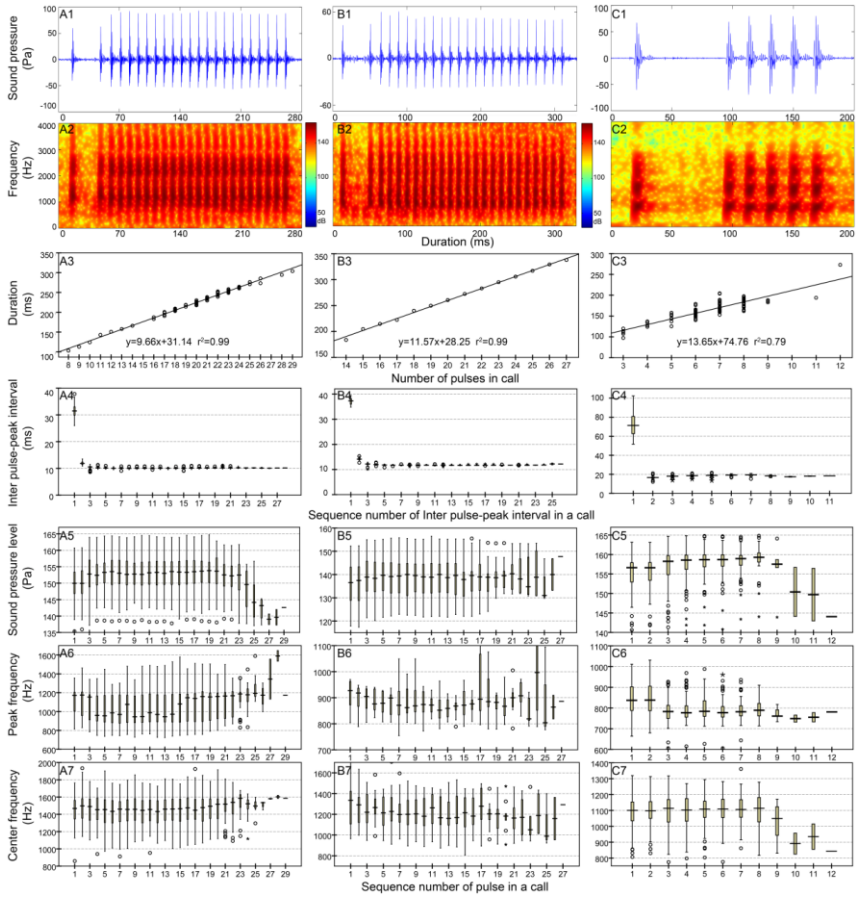

723

724 **Figure 7 Scatterplot using the canonical discriminant function (A) and dendrogram using the**
725 **hierarchical clustering method (B) of 31 extracted call types.** The "Rescaled distance cluster
726 combine" axis in B shows the distance at which the clusters combine. When creating a dendrogram,
727 SPSS rescales the actual distance between the cases to fall into a 0-25 unit range; thus, the last

merging step to a one-cluster solution occurs at a distance of 25.

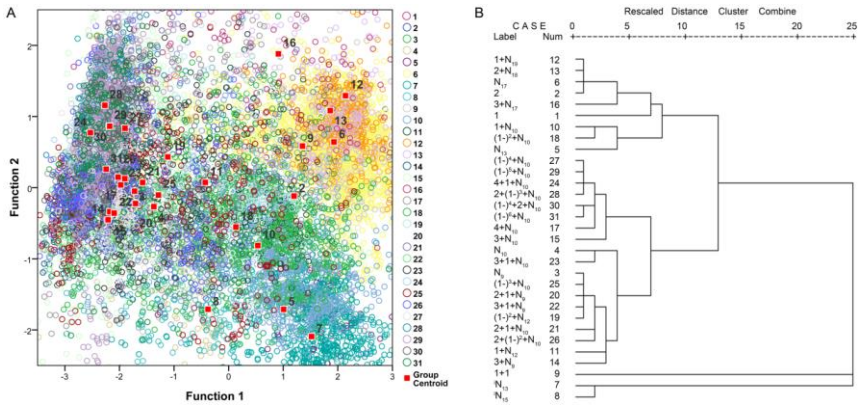

Figure 8 Occurrence pattern of the 66 call types during passive acoustic monitoring periods.

Yellow patches in the matrix indicate the corresponding call types (x-axis) observed on that day (y-axis). The number on the y-axis corresponds to the call type sequence in Table 1.

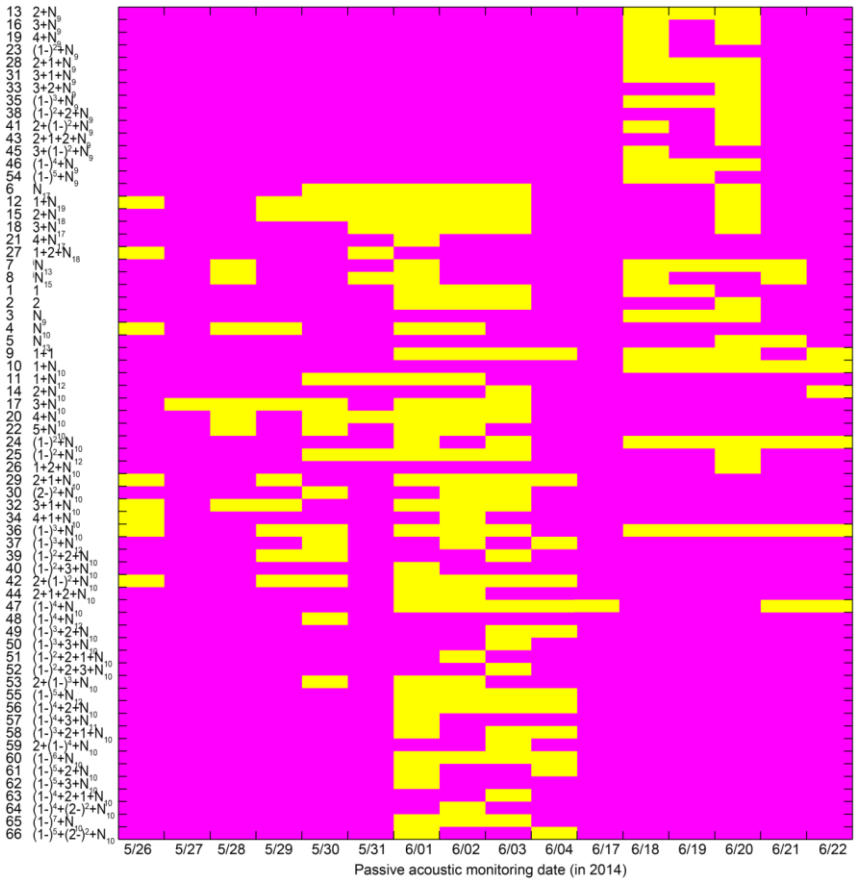
13 2+N9
16 3+N9
19 4+N9
23 (1-)2+N9
28 2+1+N9
31 3+1+N9
33 3+2+N9
35 (1-)2+N9
38 (1-)2+2+N9
41 2+(1-)2+N9
43 2+1+2+N9
45 3+(1-)2+N9
46 (1-)4+N9
54 (1-)5+N9
6 N9
12 1+N19
15 2+N18
18 3+N17
21 4+N16
27 1+2+N18
7 N13
8 N15
1 1
2 2
3 N9
4 N10
5 N12
9 1+1
10 1+N10
11 1+N12
14 2+N10
17 3+N10
20 4+N10
22 5+N10
24 (1-)2+N10
25 (1-)2+N12
26 1+2+N10
29 2+1+N10
30 (2-)2+N10
32 3+1+N10
34 4+1+N10
36 (1-)2+N10
37 (1-)3+N10
39 (1-)2+2+N10
40 (1-)2+3+N10
42 2+(1-)2+N10
44 2+1+2+N10
47 (1-)4+N10
48 (1-)4+N10
49 (1-)3+2+N10
50 (1-)2+3+N10
51 (1-)2+2+1+N10
52 (1-)2+2+3+N10
53 2+(1-)2+N10
55 (1-)5+N10
56 (1-)4+2+N10
57 (1-)4+3+N10
58 (1-)3+2+1+N10
59 2+(1-)4+N10
60 (1-)6+N10
61 (1-)5+2+N10
62 (1-)5+3+N10
63 (1-)4+2+1+N10
64 (1-)4+(2-)2+N10
65 (1-)7+N10
66 (1-)6+(2-)2+N10
5/26
5/27
5/28
5/29
5/30
5/31
6/01
6/02
6/03
6/04
6/17
6/18
6/19
6/20
6/21
6/22
Passive acoustic monitoring date (in 2014)

733

734

735 Tables

736 **Table 1 Call type classification.**

Type	Call name	No. of sections	Inter-pulsepeak interval (IPPI) pattern	Observed No. of pulses in section N
1	1	One		
2	2	One	IPPIs converged at 13 ms	
3	N_9	One	Decreasing then increasing IPPI, median at 9 ms	29-30,33-37
4	N_{10}	One	Decreasing then increasing IPPI, median at 10 ms	27-29,33-36,43,45,51
5	N_{13}	One	Nearly constant IPPI at 13 ms	3-7,9,11,12,14
6	N_{17}	One	Increasing IPPI, median at 17 ms	3-15,18
7	$^{i}N_{13}$	One	Increasing, decreasing, then increasing IPPI, median at 13 ms	2-5,9-17
8	$^{i}N_{15}$	One	Decreasing IPPI, median at 15 ms	7-11,13,15
9	1+1	Two	IPPI median at 41 ms	
10	$1+N_{10}$	Two	Nearly constant IPPI, median at 10 ms	7-13,15-25,27,28
11	$1+N_{12}$	Two	Nearly constant IPPI, median at 12 ms	13-26
12	$1+N_{19}$	Two	Increasing IPPI, median at 19 ms	2-8,10,11
13	$2+N_9$	Two	Near constant IPPI, median at 9 ms	23,25,27,28,30
14	$2+N_{10}$	Two	Near constant IPPI, median at 10 ms	19,26,27
15	$2+N_{18}$	Two	Increasing IPPI, median at 18 ms	3-8,10
16	$3+N_9$	Two	Near constant IPPI, median at 9 ms	24-26,29,30
17	$3+N_{10}$	Two	Near constant IPPI, median at 10 ms	3-11,24-25,27-34,37-39,44
18	$3+N_{17}$	Two	Increasing IPPI, median at 17 ms	4-7
19	$4+N_9$	Two	Near constant IPPI, median at 9 ms	25-27,31
20	$4+N_{10}$	Two	Near constant IPPI, median at 10 ms	3-7,15,25,28,30-31,33,35,36
21	$4+N_{17}$	Two	Increasing IPPI, median at 17 ms	6
22	$5+N_{10}$	Two	Nearly constant IPPI, median at 10 ms	3-5,7
23	$(1-)^2+N_9$	Three	Nearly constant IPPI, median at 9 ms	19,22,23
24	$(1-)^2+N_{10}$	Three	Nearly constant IPPI, median at 10 ms	2,9-24,29,30
25	$(1-)^2+N_{12}$	Three	Nearly constant IPPI, median at 12 ms	6-11,13-15,19-21
26	$1+2+N_{10}$	Three	Nearly constant IPPI, median at 10 ms	16
27	$1+2+N_{18}$	Three	Nearly constant IPPI, median at 18 ms	5,7
28	$2+1+N_9$	Three	Nearly constant IPPI, median at 9 ms	21,23-25,28,29,31,32
29	$2+1+N_{10}$	Three	Nearly constant IPPI, median at 10 ms	23,25-28,30,32,34,35,40
30	$(2-)^2+N_{10}$	Three	Nearly constant IPPI, median at 10 ms	23,26
31	$3+1+N_9$	Three	Nearly constant IPPI, median at 9 ms	23-25,27,30-32,34
32	$3+1+N_{10}$	Three	Nearly constant IPPI, median at 10 ms	27-31,33-35,37
33	$3+2+N_9$	Three	Nearly constant IPPI, median at 9 ms	26
34	$4+1+N_{10}$	Three	Nearly constant IPPI, median at 10 ms	21,29-31,33

35	$(1\text{-})^3+N_9$	Four	Nearly constant IPPI, median at 9 ms	18,21,26,29
36	$(1\text{-})^3+N_{10}$	Four	Nearly constant IPPI, median at 10 ms	1,9-14,16,17,19,23-25,27-29,31,33
37	$(1\text{-})^3+N_{12}$	Four	Nearly constant IPPIs, median at 12 ms	8,10,13
38	$(1\text{-})^2+2+N_9$	Four	Nearly constant IPPI, median at 9 ms	26,29
39	$(1\text{-})^2+2+N_{10}$	Four	Nearly constant IPPI, median at 10 ms	20,21,29
40	$(1\text{-})^2+3+N_{10}$	Four	Nearly constant IPPI, median at 10 ms	18
41	$2+(1\text{-})^2+N_9$	Four	Nearly constant IPPI, median at 9 ms	22,23
42	$2+(1\text{-})^2+N_{10}$	Four	Nearly constant IPPI, median at 10 ms	20-24,26-33,36
43	$2+1+2+N_9$	Four	Nearly constant IPPI, median at 9 ms	28
44	$2+1+2+N_{10}$	Four	Nearly constant IPPI, median at 10 ms	22,25,30
45	$3+(1\text{-})^2+N_9$	Four	Nearly constant IPPI, median at 9 ms	25
46	$(1\text{-})^4+N_9$	Five	Nearly constant IPPI, median at 9 ms	15,18,23,24
47	$(1\text{-})^4+N_{10}$	Five	Nearly constant IPPI, median at 10 ms	1,6,7,11,13,16-25,27,28
48	$(1\text{-})^4+N_{12}$	Five	Nearly constant IPPI, median at 12 ms	11
49	$(1\text{-})^3+2+N_{10}$	Five	Nearly constant IPPI, median at 10 ms	20,21
50	$(1\text{-})^3+3+N_{10}$	Five	Nearly constant IPPI, median at 10 ms	17
51	$(1\text{-})^2+2+1+N_{10}$	Five	Nearly constant IPPI, median at 10 ms	26
52	$(1\text{-})^2+2+3+N_{10}$	Five	Nearly constant IPPI, median at 10 ms	14
53	$2+(1\text{-})^3+N_{10}$	Five	Nearly constant IPPI, median at 10 ms	23-25,27,28,32
54	$(1\text{-})^5+N_9$	Six	Nearly constant IPPI, median at 9 ms	17,21
55	$(1\text{-})^5+N_{10}$	Six	Nearly constant IPPI, median at 10 ms	1,16-23,26
56	$(1\text{-})^4+2+N_{10}$	Six	Nearly constant IPPI, median at 10 ms	15,18-20,28
57	$(1\text{-})^4+3+N_{11}$	Six	Nearly constant IPPI, median at 11 ms	11
58	$(1\text{-})^3+2+1+N_{10}$	Six	Nearly constant IPPI, median at 10 ms	16,18
59	$2+(1\text{-})^4+N_{10}$	Six	Nearly constant IPPI, median at 10 ms	22
60	$(1\text{-})^6+N_{10}$	Seven	Nearly constant IPPI, median at 10 ms	14-17,19,20,24
61	$(1\text{-})^5+2+N_{10}$	Seven	Nearly constant IPPI, median at 10 ms	16-18
62	$(1\text{-})^5+3+N_{10}$	Seven	Nearly constant IPPI, median at 10 ms	16
63	$(1\text{-})^4+2+1+N_{10}$	Seven	Nearly constant IPPI, median at 10 ms	16
64	$(1\text{-})^4+(2\text{-})^2+N_{10}$	Seven	Nearly constant IPPI, median at 10 ms	20
65	$(1\text{-})^7+N_{10}$	Eight	Nearly constant IPPI, median at 10 ms	11,13,14,19,21
66	$(1\text{-})^5+(2\text{-})^2+N_{10}$	Eight	Nearly constant IPPI, median at 10 ms	9,15

For each signal, pulses with an inter-pulsepeak interval (IPPI) greater than 1.5 times the median IPPI of the signal were grouped into different sections. For signals that consisted of fewer than three pulses, pulses with an IPPI greater than 24 ms (three times the duration of a single pulse) were further grouped into different sections. In the call name column, '+' is used to separate different

sections of a call; the number denotes the number of pulses in that section; '(1-)' and '(2-)' denote repeated sections that consist of one and two pulses, respectively; the digital superscripts denote the number of repeats in the repeating section; 'N' denotes the last section of a call that varied in the number of pulses; the digital subscripts denote the median IPPIs of the last portion of the call; the subscript i denotes calls with a zero-to-peak sound pressure level of the first pulse approximately 10 dB weaker than that of the remainder within the call. For call types with more than one portion, the IPPI pattern of the last section is given.

Table 2 Descriptive statistics of sonic parameters of the N_9, N_{10}, N_{13}, and N_{17} call types.

		Dur	IPPI	$\tau_{95\%}$	τ_{-3dB}	τ_{-10dB}	f_p	f_c	BW_{rms}	Q	SPL_{zp}	SPL_{rms}	EFD	N1	N2	N3
N_9	P50	300.30	9.09	3.22	0.31	0.36	856	1366	1228	1.14	130.99	122.81	147.51	9	287	296
	QD	28.03	0.25	0.48	0.10	0.21	59	153	557	0.32	2.50	3.34	2.97			
	P5	253.39	8.32	2.42	0.15	0.16	747	1015	679	0.48	122.99	112.08	139.48			
	P95	334.04	9.49	6.49	1.24	1.53	1144	2273	4709	1.62	136.98	128.21	152.82			
N_{10}	P50	356.94	10.50	4.35	0.21	1.16	903	1580	1222	1.27	139.67	128.22	154.66	13	448	461
	QD	59.78	0.29	1.51	0.11	0.48	113	289	525	0.31	9.20	10.27	9.09			
	P5	275.72	9.73	2.93	0.11	0.15	667	1024	772	0.62	123.93	110.66	138.54			
	P95	544.98	11.07	7.39	0.43	1.72	1274	2450	3705	1.80	147.13	137.36	162.00			
N_{13}	P50	119.15	13.11	3.33	0.39	0.86	1296	1776	702	2.53	156.35	146.42	170.87	26	190	216
	QD	46.27	0.22	0.48	0.02	0.09	139	44	66	0.23	1.33	1.45	1.16			
	P5	35.06	12.67	2.54	0.34	0.72	1178	1681	595	1.23	150.66	140.18	166.38			
	P95	170.20	13.93	5.99	0.48	1.19	2390	1931	1548	2.92	158.05	147.96	172.61			
N_{17}	P50	149.11	17.44	4.40	0.52	0.97	789	1144	490	2.35	159.56	151.11	177.30	462	3803	4265
	QD	10.00	1.11	0.34	0.02	0.05	49	48	27	0.11	1.48	1.36	1.41			
	P5	141.53	16.04	4.02	0.50	0.93	765	1100	464	2.23	158.17	149.75	175.99			
	P95	179.74	19.31	5.42	0.64	1.82	957	1278	641	2.65	163.93	155.10	181.30			

P50, median; P5 and P95, 5th percentile and 95th percentile, respectively; QD, quartile deviation; Dur, duration; IPPI, inter-pulsepeak interval; $\tau_{95\%}$, duration of 95% cumulative energy; τ_{-3dB} and τ_{-10dB}, duration of -3 dB and -10 dB of the peak amplitude of the enveloped signal, respectively; f_p, peak frequency; f_c, center frequency; BW_{rms}, centralized root-mean-square bandwidth; Q, quality factor; SPL_{zp} and SPL_{rms}, zero-to-peak and root-mean-square sound pressure levels, respectively;

EFD, energy flux density; N1, N2 and N3, number of calls, inter-pulsepeak intervals and pulses analyzed, respectively. The duration is in seconds, the frequency is in Hz, the SPL is in dB re 1 µPa, and the EFD is in dB re 1µPa^{2}s. The IPIs are not shown here and can be obtained by subtracting 8 ms from the IPPIs. The same notation was used for the following tables.

Table 3 Descriptive statistics of sonic parameters of the $^{i}N_{13}$ and $^{i}N_{15}$ call types.

		Dur	IPPI	$\tau_{95\%}$	τ_{-3dB}	τ_{-10dB}	f_p	f_c	BW_{rms}	Q	SPL_{zp}	SPL_{rms}	EFD	N1	N2	N3
$^{i}N_{13}$	P50	174.10	13.15	3.17	0.39	0.82	1490	1770	663	2.66	157.38	147.01	171.91	111	1266	1377
	QD	17.49	0.35	0.42	0.03	0.13	217	49	52	0.22	2.09	2.05	1.91			
	P5	33.26	12.35	2.42	0.33	0.45	1184	1601	545	1.54	146.21	135.78	162.38			
	P95	202.23	15.37	5.75	0.60	1.31	2390	1930	1038	3.29	161.03	151.31	175.66			
$^{i}N_{15}$	P50	169.31	14.96	3.12	0.41	0.42	1510	1787	929	1.95	142.26	133.21	157.60	16	158	174
	QD	19.04	1.51	0.33	0.10	0.15	167	47	122	0.22	2.89	2.47	2.69			
	P5	139.67	13.55	2.70	0.24	0.20	1283	1750	823	1.70	140.50	131.32	155.86			
	P95	192.87	19.30	5.30	0.57	0.65	2202	2362	2059	2.98	152.37	143.35	167.28			

Table 4 Descriptive statistics of sonic parameters of the 1+N_{10}, 1+N_{12} and 1+N_{19} call types.

		Dur	IPPI	$\tau_{95\%}$	τ_{-3dB}	τ_{-10dB}	f_p	f_c	BW_{rms}	Q	SPL_{zp}	SPL_{rms}	EFD	N1	N2	N3
1+N_{10}	P50	232.80	10.15	3.42	0.41	1.08	1128	1474	669	2.12	152.67	143.04	167.93	75	1432	1507
	QD	22.34	0.18	0.59	0.04	0.42	144	122	84	0.30	3.43	3.29	3.50			
	P5	124.18	9.82	2.20	0.33	0.38	792	1148	550	0.97	141.26	132.09	157.57			
	P95	278.07	27.17	6.19	0.58	1.56	1355	1708	1385	2.80	161.00	150.70	175.61			
1+N_{12}	P50	260.67	11.73	3.30	0.40	0.43	879	1213	684	1.67	138.77	130.44	155.31	15	292	307
	QD	41.74	0.19	0.64	0.05	0.25	41	130	227	0.48	7.49	6.98	6.34			
	P5	183.67	11.55	2.23	0.19	0.20	796	935	525	0.67	122.02	112.12	138.95			
	P95	337.81	35.09	5.44	0.90	1.35	1193	1516	2284	2.34	154.90	144.12	170.29			
1+N_{19}	P50	165.96	18.73	4.64	0.52	1.01	789	1105	480	2.33	157.80	149.44	175.92	105	591	696

	QD	14.61	0.99	0.36	0.03	0.13	42	62	33	0.16	2.05	2.20	2.12			
	P5	115.74	15.75	3.71	0.49	0.89	722	898	395	1.15	144.06	135.10	163.23			
	P95	195.68	79.77	6.87	0.79	3.04	946	1254	895	2.61	162.68	153.89	180.29			

760

761 **Table 5 Frequency and inter-pulsepeak interval (IPPI) characteristics of soniferous fish in the Pearl River Estuary.**

Family	Species	Latin name	Condition	Peak frequency	IPPI	First IPPI	Last IPPI	Comments	Reference
Sciaenidae	Belanger's croaker	*Johnius belangerii*	Voluntary	500-1000 Hz[a]		40 ms	20 ms[e]		Pilleri et al. 1982
				750-1250Hz				long burst	Pilleri et al. 1982
			Disturbance	584±181 Hz	12.9 ms	14.4 ms	16.9 ms		Mok et al. 2011
	Big-snout croaker	*J. macrorhynus*	Voluntary	1146±131 Hz		40.1 ms	9.7 ms[e]	purr signals[c]	Lin et al. 2007
			Voluntary	1050±84 Hz		35.3 ms	10.4 ms[e]	purr signal[d]	Lin et al. 2007
			Voluntary	1133±119 Hz	36.7 ms			dual-knocks[c]	Lin et al. 2007
			Voluntary	1135±85 Hz	39.4 ms			dual-knocks[d]	Lin et al. 2007
			Disturbance	808±142 Hz		22.2 ms	9.5 ms[e]	purr signals	Lin et al. 2007
	Big-snout croaker	*J. macrorhynus*	Disturbance	807±143 Hz	10.1	22.2 ms	10.5 ms		Mok et al. 2011
	Sciaenidae	*J. distincus*	Disturbance	839±144 Hz		9.97±0.72 ms	12.36±0.53 ms	male	Tsai 2009
				581±66 Hz		10.12±0.82 ms	12.53±0.79 ms	female	Tsai 2009
					10.8 ms	11.1ms	12.3ms		Mok et al. 2011
	Sin croaker	*J. dussumieri*	Disturbance	517 Hz		11.4 ms	14.9 ms		Tsai 2009
	White croaker	*Pennahia argentata*	Voluntary	457 Hz				male	Ramcharitar et al. 2006
			Voluntary	267 Hz				female	Ramcharitar et al. 2006
			Disturbance	543±98 Hz	22.9 ms	24.0 ms	37.9 ms		Mok et al. 2011
	Greyfin croaker	*P. anea*	Disturbance	736±115 Hz	10.6 ms	9.1 ms	12.1 ms		Mok et al. 2011
	Bighead white croaker	*P. macrocephalus*	Disturbance	576±93 Hz	34.6 m	25.2 ms	38.1 ms		Mok et al. 2011
	Pawak croaker	*P. pawak*	Disturbance	736±101 Hz	9.1 ms	8.5 ms	9.7 ms		Mok et al. 2011
	Large yellow croaker	*Pseudosciaena crocea*	Voluntary	550-750 Hz[a]				single pulse	Liu et al. 2010
			Voluntary	800-850 Hz[a]	90-150 ms[a]			2-3 pulse signal	Ren et al. 2007
			Disturbance	800-850 Hz[a]	>30ms[a]			2-5 pulse signal	Liu et al. 2010
	Southern meagre	*Argyrosomus japonicas*	Voluntary	686±203 Hz	24±3 ms			male	Ueng et al. 2007

			Voluntary	587±190 Hz	23±3 ms			female	Ueng et al. 2007
	Yellow Drum	*Nibea albiflora*	Voluntary	650±20 Hz					Ren et al. 2007
	Reeve's croaker	*N. acuta*	Voluntary	630±15 Hz					Ren et al. 2007
			Disturbance	<500 Hz[a]					Tsai 2009
	Tiger-toothed croaker	*Otolithes ruber*	Disturbance	354-1717 Hz[a]	8.3-12.2 ms[a]				Mok et al. 2011
	Blackmouth croaker	*Atrobucca nibe*	Disturbance		47.0-57.8 ms[a]				Mok et al. 2011
Trichiuridae	Cutlassfish	*Trichiurus haumela*	Voluntary	628±11 Hz					Ren et al. 2007
Pristigasteridae	Elongate ilisha	*Ilisha elongata*	Voluntary	251±18 Hz					Ren et al. 2007
Ariidae	Sea catfish	*Arius sp.*	Voluntary	735±12 Hz					Ren et al. 2007
		A. maculates	Disturbance		0.47-4.33 ms[ab]			5-11 pulse signal	Mok et al. 2011
Glaucosomatidae	Pearl perch	*Glaucosoma buergeri*	Disturbance		30 ms			2-9 pulse signal	Mok et al. 2011b
Priacanthidae	Bigeye snapper	*Priacanthus macracanthus*	Disturbance	172 Hz	15.9 ms				Tsai 2009
Terapontidae	Trumpeter perch	*Pelates quadrilineatus*	Disturbance	690±171 Hz	4 ms				Tsai 2009
Haemulidae	Javelin grunter	*Pomadasys kaakan*	Disturbance		94.1 ms				Tsai 2009

762 Except when mentioned, the results are given as the mean or mean ±standard deviation(sd).

763 The superscript a denotes results given in a range.

764 The superscript b denotes results given for the inter-pulse interval.

765 The superscript c denotes results recorded in the field.

766 The superscript d denotes results recorded in a large aquarium.

767 The superscripts e denotes results that are the mean of all the IPPIs except the first IPPI.

Supporting information

Fig. S1 Characteristic of the (A) 2 and (B) 1+1 call types. Rows 1 and 2 are the oscillogram and sonogram, respectively, of a representative signal for each call type. Row 3 is the duration of a call as a function of the number of pulses within the call. Rows 4 is the pooled inter-pulsepeak interval of each pulse versus the order at which it occurs within a call. For the boxplot, the line inside the box indicates the median value, and the upper and lower box borders are the first and third quartiles, respectively. The length of the box is the interquartile range (IQR). The whiskers extend to the most extreme data within the limit of 1.5 IQRs from the end of the box. Open circles (o) denote mild outliers with values greater than 1.5 IQRs but fewer than 3 IQRs from the end of the box. Asterisks (*) denote extreme outliers with values greater than 3 box lengths from the upper or lower edges of the box. Sonogram configuration: FFT size, 96,000; window type, Hanning; overlap samples per frame, 95%.

Table S1 Descriptive statistics of the sonic parameters of single and paired pulse call types. P50, median; P5 and P95, 5th percentile and 95th percentile, respectively; QD, quartile deviation; Dur, duration; IPPI, inter-pulsepeak interval; $\tau_{95\%}$, duration of 95% cumulative energy; τ_{-3dB} and τ_{-10dB}, duration of -3 dB and -10 dB of the peak amplitude of the enveloped signal, respectively; f_p, peak frequency; f_c, center frequency; BW_{rms}, centralized root-mean-square bandwidth; Q, quality factor; SPL_{zp} and SPL_{rms}, zero-to-peak and root-mean-square sound pressure levels, respectively; EFD, energy flux density; N1, N2 and N3, number of calls, inter-pulsepeak intervals and pulses analyzed, respectively. The duration is in seconds, the frequency is in Hz, the SPL is in dB re 1 μPa, and the EFD is in dB re 1μPa^2s. The IPIs are not shown here and can be obtained by subtracting 8 ms from the IPPIs. The same notation was used for the following tables.

Fig. S2 Characteristic of the (A) 2+N_9, (B) 2+N_{10} and (C) 2+N_{18} call types. Rows 1 and 2 are the oscillogram and sonogram, respectively, of a representative signal for each call type. Row 3 is the duration of a call as a function of the number of pulses within the call. Rows 4 is the pooled inter-pulsepeak interval of each pulse versus the order at which it occurs within a call.

Table S2 Descriptive statistics of sonic parameters of the 2+N_9, 2+N_{10} and 2+N_{18} call types.

Fig. S3 Characteristic of the (A) 3+N_9, (B) 3+N_{10} and (C) 3+N_{17} call types. Rows 1 and 2 are the oscillogram and sonogram, respectively, of a representative signal for each call type. Row 3 is the duration of a call as a function of the number of pulses within the call. Rows 4 is the pooled inter-pulsepeak interval of each pulse versus the order at which it occurs within a call.

Table S3 Descriptive statistics of sonic parameters of the 3+N_9, 3+N_{10} and 3+N_{17} call types.

Fig. S4 Characteristic of the (A) 4+N_9, (B) 4+N_{10} and (C)4+N_{17} call types. Rows 1 and 2 are the oscillogram and sonogram, respectively, of a representative signal for each call type. Row 3 is the duration of a call as a function of the number of pulses within the call. Rows 4 is the pooled inter-pulsepeak interval of each pulse versus the order at which it occurs within a call.

Table S4 Descriptive statistics of sonic parameters of the 4+N_9, 4+N_{10} and 4+N_{17} call types.

Fig. S5 Characteristic of the 5+N_{10} call type. Rows 1 and 2 are the oscillogram and sonogram, respectively, of a representative signal for each call type. Row 3 is the duration of a call as a function of the number of pulses within the call. Rows 4 is the pooled inter-pulsepeak interval of each pulse versus the order at which it occurs within a call.

Table S5 Descriptive statistics of sonic parameters of 5+N_{10} call type.

Fig. S6 Characteristic of the (A) (1-)^2+N_9, (B) (1-)^2+N_{10} and (C) (1-)^2+N_{12} call type. Rows 1 and 2 are the oscillogram and sonogram, respectively, of a representative signal for each call type. Row

3 is the duration of a call as a function of the number of pulses within the call. Rows 4 is the pooled inter-pulsepeak interval of each pulse versus the order at which it occurs within a call.

Table S6 Descriptive statistics of sonic parameters of the $(1-)^2+N_9$, $(1-)^2+N_{10}$ and $(1-)^2+N_{12}$ call types.

Fig. S7 Characteristic of the (A) $1+2+N_{10}$ and (B) $1+2+N_{18}$ call types. Rows 1 and 2 are the oscillogram and sonogram, respectively, of a representative signal for each call type. Row 3 is the duration of a call as a function of the number of pulses within the call. Rows 4 is the pooled inter-pulsepeak interval of each pulse versus the order at which it occurs within a call.

Table S7 Descriptive statistics of sonic parameters of the $1+2+N_{10}$ and $1+2+N_{18}$ call types.

Fig. S8 Characteristic of the (A) $2+1+N_9$ and (B) $2+1+N_{10}$ call types. Rows 1 and 2 are the oscillogram and sonogram, respectively, of a representative signal for each call type. Row 3 is the duration of a call as a function of the number of pulses within the call. Rows 4 is the pooled inter-pulsepeak interval of each pulse versus the order at which it occurs within a call.

Table S8 Descriptive statistics of sonic parameters of the $2+1+N_9$ and $2+1+N_{10}$ call types.

Fig. S9 Characteristic of the (A) $(2-)^2+N_{10}$ and (B) $4+1+N_{10}$ call types. Rows 1 and 2 are the oscillogram and sonogram, respectively, of a representative signal for each call type. Row 3 is the duration of a call as a function of the number of pulses within the call. Rows 4 is the pooled inter-pulsepeak interval of each pulse versus the order at which it occurs within a call.

Table S9 Descriptive statistics of sonic parameters of the $(2-)^2+N_{10}$ and $4+1+N_{10}$ call types.

Fig. S10 Characteristic of the (A) $3+1+N_9$ and (B) $3+1+N_{10}$ call types. Rows 1 and 2 are the oscillogram and sonogram, respectively, of a representative signal for each call type. Row 3 is the duration of a call as a function of the number of pulses within the call. Rows 4 is the pooled inter-pulsepeak interval of each pulse versus the order at which it occurs within a call.

Table S10 Descriptive statistics of sonic parameters of the $3+1+N_9$ and $3+1+N_{10}$ call types.

Fig. S11 Characteristic of the (A) 3+2+N_9 and (B) 3+(1-)^2+N_9 call types. Rows 1 and 2 are the oscillogram and sonogram, respectively, of a representative signal for each call type. Row 3 is the duration of a call as a function of the number of pulses within the call. Rows 4 is the pooled inter-pulsepeak interval of each pulse versus the order at which it occurs within a call.

Table S11 Descriptive statistics of sonic parameters of the 3+2+N_9 and 3+(1-)^2+N_9 call types.

Fig. S12 Characteristic of the (A) (1-)^3+N_9, (B) (1-)^3+N_{10} and (C) (1-)^3+N_{12} call types. Rows 1 and 2 are the oscillogram and sonogram, respectively, of a representative signal for each call type. Row 3 is the duration of a call as a function of the number of pulses within the call. Rows 4 is the pooled inter-pulsepeak interval of each pulse versus the order at which it occurs within a call.

Table S12 Descriptive statistics of sonic parameters of the (1-)^3+N_9, (1-)^3+N_{10} and (1-)^3+N_{12} call types.

Fig. S13 Characteristic of the (A) (1-)^2+2+N_9 and (B) (1-)^2+2+N_{10} call types. Rows 1 and 2 are the oscillogram and sonogram, respectively, of a representative signal for each call type. Row 3 is the duration of a call as a function of the number of pulses within the call. Rows 4 is the pooled inter-pulsepeak interval of each pulse versus the order at which it occurs within a call.

Table S13 Descriptive statistics of sonic parameters of the (1-)^2+2+N_9 and (1-)^2+2+N_{10} call types.

Fig. S14 Characteristic of the (1-)^2+3+N_{10} call type. Rows 1 and 2 are the oscillogram and sonogram, respectively, of a representative signal for each call type. Row 3 is the duration of a call as a function of the number of pulses within the call.

Table S14 Descriptive statistics of sonic parameters of the (1-)^2+3+N_{10} call type.

Fig. S15 Characteristic of the (A) 2+(1-)^2+N_9 and (B) 2+(1-)^2+N_{10} call types. Rows 1 and 2 are the oscillogram and sonogram, respectively, of a representative signal for each call type. Row 3 is the duration of a call as a function of the number of pulses within the call. Rows 4 is the pooled inter-pulsepeak interval of each pulse versus the order at which it occurs within a call.

Table S15 Descriptive statistics of sonic parameters of the $2+(1-)^2+N_9$ and $2+(1-)^2+N_{10}$ call types.

Fig. S16 Characteristic of the (A) $2+1+2+N_9$ and (B) $2+1+2+N_{10}$ call types. Rows 1 and 2 are the oscillogram and sonogram, respectively, of a representative signal for each call type. Row 3 is the duration of a call as a function of the number of pulses within the call. Rows 4 is the pooled inter-pulsepeak interval of each pulse versus the order at which it occurs within a call.

Table S16 Descriptive statistics of sonic parameters of the $2+1+2+N_9$ and $2+1+2+N_{10}$ call types.

Fig. S17 Characteristic of the (A) $(1-)^4+N_9$, (B) $(1-)^4+N_{10}$ and (C) $(1-)^4+N_{12}$ call types. Rows 1 and 2 are the oscillogram and sonogram, respectively, of a representative signal for each call type. Row 3 is the duration of a call as a function of the number of pulses within the call. Rows 4 is the pooled inter-pulsepeak interval of each pulse versus the order at which it occurs within a call.

Table S17 Descriptive statistics of sonic parameters of the $(1-)^4+N_9$, $(1-)^4+N_{10}$ and $(1-)^4+N_{12}$ call types.

Fig. S18 Characteristic of the (A) $(1-)^3+2+N_{10}$ and (B) $(1-)^3+3+N_{10}$ call types. Rows 1 and 2 are the oscillogram and sonogram, respectively, of a representative signal for each call type. Row 3 is the duration of a call as a function of the number of pulses within the call. Rows 4 is the pooled inter-pulsepeak interval of each pulse versus the order at which it occurs within a call.

Table S18 Descriptive statistics of sonic parameters of the $(1-)^3+2+N_{10}$ and $(1-)^3+3+N_{10}$ call types.

Fig. S19 Characteristic of the (A) $(1-)^2+2+1+N_{10}$ and (B) $(1-)^2+2+3+N_{10}$ call types. Rows 1 and 2 are the oscillogram and sonogram, respectively, of a representative signal for each call type. Row 3 is the duration of a call as a function of the number of pulses within the call.

Table S19 Descriptive statistics of sonic parameters of the $(1-)^2+2+1+N_{10}$ and $(1-)^2+2+3+N_{10}$ call types.

Fig. S20 Characteristic of the (A) $2+(1-)^3+N_{10}$ and (B) $2+(1-)^4+N_{10}$ call types. Rows 1 and 2 are the oscillogram and sonogram, respectively, of a representative signal for each call type. Row 3 is the duration of a call as a function of the number of pulses within the call. Rows 4 is the pooled

inter-pulsepeak interval of each pulse versus the order at which it occurs within a call.

Table S20 Descriptive statistics of sonic parameters of the 2+(1-)^3+N$_{10}$ and 2+(1-)^4+N$_{10}$ call types.

Fig. S21 Characteristic of the (A) (1-)^5+N$_9$ and (B) (1-)^5+N$_{10}$ call types. Rows 1 and 2 are the oscillogram and sonogram, respectively, of a representative signal for each call type. Row 3 is the duration of a call as a function of the number of pulses within the call. Rows 4 is the pooled inter-pulsepeak interval of each pulse versus the order at which it occurs within a call.

Table S21 Descriptive statistics of sonic parameters of the (1-)^5+N$_9$ and (1-)^5+N$_{10}$ call types.

Fig. S22 Characteristic of the (A) (1-)^4+2+N$_{10}$ and (B) (1-)^4+3+N$_{11}$ call types. Rows 1 and 2 are the oscillogram and sonogram, respectively, of a representative signal for each call type. Row 3 is the duration of a call as a function of the number of pulses within the call. Rows 4 is the pooled inter-pulsepeak interval of each pulse versus the order at which it occurs within a call.

Table S22 Descriptive statistics of sonic parameters of the(1-)^4+2+N$_{10}$ and (1-)^4+3+N$_{11}$ call types.

Fig. S23 Characteristic of the (A) (1-)^3+2+1+N$_{10}$ and (B) (1-)^4+2+1+N$_{10}$ call types. Rows 1 and 2 are the oscillogram and sonogram, respectively, of a representative signal for each call type. Row 3 is the duration of a call as a function of the number of pulses within the call. Rows 4 is the pooled inter-pulsepeak interval of each pulse versus the order at which it occurs within a call.

Table S23 Descriptive statistics of sonic parameters of the (1-)^3+2+1+N$_{10}$ and (1-)^4+2+1+N$_{10}$ call types.

Fig. S24 Characteristic of the (A) (1-)^6+N$_{10}$ and (B) (1-)^7+N$_{10}$ call types. Rows 1 and 2 are the oscillogram and sonogram, respectively, of a representative signal for each call type. Row 3 is the duration of a call as a function of the number of pulses within the call. Rows 4 is the pooled inter-

pulsepeak interval of each pulse versus the order at which it occurs within a call.

Table S24 Descriptive statistics of sonic parameters of the $(1\text{-})^6+N_{10}$ and $(1\text{-})^7+N_{10}$ call types.

Fig. S25 Characteristic of the (A) $(1\text{-})^5+2+N_{10}$ and (B) $(1\text{-})^5+3+N_{10}$ call types. Rows 1 and 2 are the oscillogram and sonogram, respectively, of a representative signal for each call type. Row 3 is the duration of a call as a function of the number of pulses within the call. Rows 4 is the pooled inter-pulsepeak interval of each pulse versus the order at which it occurs within a call.

Table S25 Descriptive statistics of sonic parameters of the $(1\text{-})^5+2+N_{10}$ and $(1\text{-})^5+3+N_{10}$ call types.

Fig. S26 Characteristic of the (A) $(1\text{-})^4+(2\text{-})^2+N_{10}$ and (B) $(1\text{-})^5+(2\text{-})^2+N_{10}$ call types. Rows 1 and 2 are the oscillogram and sonogram, respectively, of a representative signal for each call type. Row 3 is the duration of a call as a function of the number of pulses within the call. Rows 4 is the pooled inter-pulsepeak interval of each pulse versus the order at which it occurs within a call.

Table S26 Descriptive statistics of sonic parameters of the $(1\text{-})^4+(2\text{-})^2+N_{10}$ and $(1\text{-})^5+(2\text{-})^2+N_{10}$ call types.

Fig. S27 Distribution pattern of the inter-pulspeak interval of each pulse versus the order at which it occurs within a call of all N_9 and N_{10} call types.